

Validation of CFD Codes for Propulsion System Components

by

Chun Ngok Chan

Project submitted to the faculty of the

Virginia Polytechnic Institute and State University

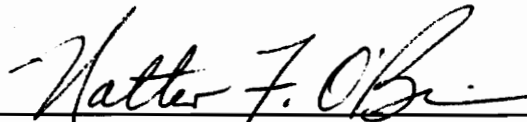
in partial fulfillment of the requirements for the degree of

Master of Engineering

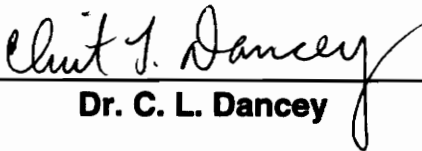
in

Mechanical Engineering

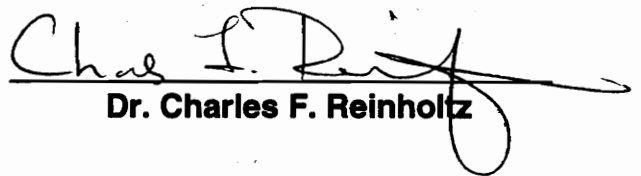
APPROVED:



Dr. Walter F. O'Brien, Chairman



Dr. C. L. Dancey



Dr. Charles F. Reinholz

December, 1996

Blacksburg, Virginia

C.2

LD
5655
V851
1996
C436
C.2

Validation of CFD Codes for Propulsion System Components

by

Chun Ngok Chan

Dr. Walter F. O'Brien, Chairman

Mechanical Engineering

(Abstract)

This report describes an international effort to investigate the present limitations of some of the commercially available CFD codes and their models. This investigation involves comparing the predictions from these codes with the experimental results of the two selected test cases. The data collection method is briefly described followed by a detailed discussion of the graphical approach used by the group of investigators to compare results. In addition, an attempt to investigate the deviation of the collected results with the experimental data is discussed.

ACKNOWLEDGMENTS

Any form of undertaking without a strong foundation can only be deemed as weak and frivolous. The individuals cited below are recognized for their contributions in building my ethical and professional mechanical engineering foundation.

First, I must acknowledge that my source of motivation in graduate school has always been my mother, Kin-Foon Chee, whose love and encouragement propelled me through my years in school. She insisted that hard work and dedication are the keys to success.

To my girlfriend, Dung Nguyen, whose constant encouragement led me through my most difficult times. Her patience and understanding gave me the strength to work hard and complete my graduate education.

To my advisor, Dr. Walter O'Brien, whose guidance and patience made me proud to be working for him. His timely advice led me through sixteen of the most grueling months I have ever experienced. I could only dream of having such a wonderful supervisor in my future endeavor.

My sincere gratitude must be extended to Dr. Clint Dancey and Dr. Charles Reinholtz for their advice and agreeing to be on the committee for this project. Also, my deepest appreciation to Dr. Myklebust for the opportunity to work as his Teaching Assistant. There is nobody I would rather assist and I enjoyed interacting with the students in his class.

I highly value my friendship with my fellow graduate students and friends at Virginia Tech. To Shaun Boller, Tony DiPietro, Michael Grose and Carlos Rodriguez for

being there when I needed help at the Turbolab. Your constant advices and timely encouragement kept me from falling behind in my project. To Joseph Cahill for being the best of friends at Virginia Tech. I would not survive the intensity of graduate school without your help.

Finally, I would like to extend my thanks to the Virginia Tech Department of Mechanical Engineering for the opportunity to attend Graduate School and work with such wonderful students and faculties.

Table of Contents

Chapter 1 Introduction	1
1.1 Project Background	1
1.2 Objective	2
Chapter 2 Test Cases and Working Group	3
2.1 Overview	3
2.2 NASA Rotor 37	3
2.3 DLR Turbine Stator Test Case	4
2.4 Working Group Members	4
Chapter 3 Apparatus and Procedure	6
3.1 Overview	6
3.2 Data Collection Methods	6
3.3 Data Visualization	7
3.4 Error Analysis	8
3.4.1 Collecting Data for Error Analysis	8
3.4.2 Method of Analysis	9
Chapter 4 Results	12
4.1 Types of Results	12
4.2 Results for the NASA Rotor 37 Test Case	13
4.3 Results for the DLR Turbine Stator Test Case	19
4.4 Results from the Error Analysis	26
Chapter 5 Discussion of Results	47
5.1 Discussion Overview	47
5.2 NASA Rotor 37 Test Case	49
5.3 DLR Turbine Stator Test Case	50
5.4 Summary	52
Chapter 6 Conclusions and Recommendations	54
6.1 Conclusions	54
6.2 Recommendations	54
References	56
Appendix A: Illustrations for Circumferential Flow Angle and Radial Flow Angle	57
Appendix B: Sample Code in Fortran for Data Manipulation and Sample Data File in TECPLOT Format	58

Appendix B.1: List of Sample Code in Fortran for Data Manipulation	58
Appendix B.2: Sample Data File in TECPLOT Format	59
Appendix C: Tables of Linearly Interpolated Data for Error Analysis	61
Vita	64

List of Illustrations

Figure 4.1:	NASA Rotor 37 Test Case: Overall Pressure Ratio vs. Normalized Mass Flow	14
Figure 4.2:	NASA Rotor 37 Test Case: Overall Efficiency vs. Normalized Mass Flow	15
Figure 4.3:	NASA Rotor 37 Test Case: Spanwise Distribution of Total Pressure	16
Figure 4.4:	NASA Rotor 37 Test Case: Spanwise Distribution of Total Temperature	17
Figure 4.5:	NASA Rotor 37 Test Case: Spanwise Distribution of Adiabatic Efficiency	18
Figure 4.6:	DLR Turbine Stator Test Case: Pitchwise Averaged Exit Circumferential Flow Angles at $X/C_x = 1.40$	19
Figure 4.6a:	DLR Turbine Stator Test Case: Pitchwise Averaged Exit Circumferential Flow Angles at $X/C_x = 1.40$	21
Figure 4.7:	DLR Turbine Stator Test Case: Pitchwise Averaged Exit Radial Flow Angles at $X/C_x = 1.40$	22
Figure 4.8:	DLR Turbine Stator Test Case: Pitchwise Averaged Exit Mach Number at $X/C_x = 1.40$	23
Figure 4.9:	DLR Turbine Stator Test Case: Pitchwise Averaged P_t/P_{o1} at $X/C_x = 1.40$	24
Figure 4.10:	DLR Turbine Stator Test Case: Pitchwise Averaged P_o/P_{o1} at $X/C_x = 1.40$	25
Figure 4.11:	NASA Rotor 37 Test Case: Difference (Deviation) between experimental and predicted values for Overall Pressure Ratio vs. Normalized Mass Flow Data	27
Figure 4.12:	NASA Rotor 37 Test Case: Percentage Difference (Deviation) between experimental and predicted values for Overall Pressure Ratio vs. Normalized Mass Flow Data	28
Figure 4.13:	NASA Rotor 37 Test Case: Difference (Deviation) between experimental and predicted values for Overall Efficiency vs. Normalized Mass Flow Data	29
Figure 4.14:	NASA Rotor 37 Test Case: Percentage Difference (Deviation) between experimental and predicted values for Overall Efficiency vs. Normalized Mass Flow Data	30
Figure 4.15:	NASA Rotor 37 Test Case: Difference (Deviation) between experimental and predicted values for Spanwise Distribution of Total Pressure Data	31
Figure 4.16:	NASA Rotor 37 Test Case: Percentage Difference (Deviation) between experimental and predicted values for Spanwise Distribution of Total Pressure Data	32
Figure 4.17:	NASA Rotor 37 Test Case: Difference (Deviation) between experimental and predicted values for Spanwise Distribution of Total Temperature Data	33

Figure 4.18: NASA Rotor 37 Test Case: Percentage Difference (Deviation) between experimental and predicted values for Spanwise Distribution of Total Temperature Data	34
Figure 4.19: NASA Rotor 37 Test Case: Difference (Deviation) between experimental and predicted values for Spanwise Distribution of Adiabatic Efficiency Data	35
Figure 4.20: NASA Rotor 37 Test Case: Percentage Difference (Deviation) between experimental and predicted values for Spanwise Distribution of Adiabatic Efficiency Data	36
Figure 4.21: DLR Turbine Stator Test Case: Difference (Deviation) between experimental and predicted values for Pitchwise Exit Circumferential Flow Angles Data	37
Figure 4.22: DLR Turbine Stator Test Case: Percentage Difference (Deviation) between experimental and predicted values for Pitchwise Exit Circumferential Flow Angles Data	38
Figure 4.23: DLR Turbine Stator Test Case: Difference (Deviation) between experimental and predicted values for Pitchwise Exit Radial Flow Angles Data	39
Figure 4.24: DLR Turbine Stator Test Case: Percentage Difference (Deviation) between experimental and predicted values for Pitchwise Exit Radial Flow Angles Data	40
Figure 4.25: DLR Turbine Stator Test Case: Difference (Deviation) between experimental and predicted values for Pitchwise Exit Mach Number Data	41
Figure 4.26: DLR Turbine Stator Test Case: Percentage Difference (Deviation) between experimental and predicted values for Pitchwise Exit Mach Number Data	42
Figure 4.27: DLR Turbine Stator Test Case: Difference (Deviation) between experimental and predicted values for Pitchwise Static Pressure Ratio Data	43
Figure 4.28: DLR Turbine Stator Test Case: Percentage Difference (Deviation) between experimental and predicted values for Pitchwise Static Pressure Ratio Data	44
Figure 4.29: DLR Turbine Stator Test Case: Difference (Deviation) between experimental and predicted values for Pitchwise Total Pressure Ratio Data	45
Figure 4.30: DLR Turbine Stator Test Case: Percentage Difference (Deviation) between experimental and predicted values for Pitchwise Total Pressure Ratio Data	46
Figure A.1: Front View of an Axial Flow Turbomachinery with Radial Flow Angle, ϕ . (V_m , V_r and V_x in the velocity triangle are absolute meridional, radial and axial velocities respectively.)	57
Figure A.2: Cross Sectional View of an Axial Flow Turbomachinery with Circumferential Flow Angle, θ . (r is the radial reference axis.)	57

List of Tables

Table 2.1	Investigators involved in the AGARD WG-26 exercise	5
Table 5.1	Mean of the mean for the error analysis of NASA Rotor 37 Test Case	48
Table 5.2	Mean of the mean for the error analysis of DLR Turbine Stator Test Case	48
Table C.1	Linearly Interpolated data from Overall Pressure vs. Normalized Mass Flow data for NASA Rotor 37 using TECPLOT	61
Table C.2	Linearly Interpolated data from Overall Efficiency vs. Normalized Mass Flow data for NASA Rotor 37 using TECPLOT	61
Table C.3	Linearly Interpolated data from Total Pressure vs. Percentage Span data for NASA Rotor 37 using TECPLOT	61
Table C.4	Linearly Interpolated data from Total Temperature vs. Percentage Span data for NASA Rotor 37 using TECPLOT	61
Table C.5	Linearly Interpolated data from Adiabatic Efficiency vs. Percentage Span data for NASA Rotor 37 using TECPLOT	62
Table C.6	Linearly Interpolated data from Pitchwise Exit Circumferential Flow Angles data for DLR Turbine Stator using TECPLOT	62
Table C.7	Linearly Interpolated data from Pitchwise Exit Radial Flow Angles data for DLR Turbine Stator using TECPLOT	62
Table C.8	Linearly Interpolated data from Pitchwise Exit Mach Number data for DLR Turbine Stator using TECPLOT	63
Table C.9	Linearly Interpolated data from Pitchwise Static Pressure Ratio data for DLR Turbine Stator using TECPLOT	63
Table C.10	Linearly Interpolated data from Pitchwise Total Pressure Ratio data for DLR Turbine Stator using TECPLOT	63

Chapter 1: Introduction

1.1 Project Background

The evolution of large computers in recent years has allowed the development of many sophisticated computational codes to predict fluid flow through engine components. These codes provide investigators with approximations of the flow field and fluid thermodynamic properties of the flow. Many engine manufacturers are already using these codes to help predict engine performances for their designs to reduce the cost and time involved in experimental testings. These codes also provide investigators with an option to change or modify their configuration for their design without having to construct experiments to test their new configurations as in the past. It must be noted however, that the results generated from these computational codes lack precision. Therefore, validation methods must be applied to evaluate the accuracy of these results.

As there are many codes utilizing different computational fluid dynamics (CFD) approaches and turbulence models, it is essential to validate these codes and their turbulence models by assessing their uncertainty margins. An international effort is needed to evaluate this problem for the purpose of improving engine design, reducing engine designing cost, and enhancing both software and hardware reliability. This problem perfectly defines the goal of Advisory Group for Aerospace Research and Development (AGARD) Working Group 26 (WG-26), which is to study the effectiveness of methods in CFD codes by means of comparing predictions from these codes with experimental results. Findings from this Working Group will be published in the final report entitled “Validation of CFD Codes for Propulsion System Components.”

Two experimental turbomachinery test cases were selected for comparison. Participation in the Working Group will require the 3-dimensional, viscous, steady-state computation of at least one of the two test cases. Results from members of the Working Group will be compared with the available experimental data. The final paper will be comprised of conclusions and recommendations that may be drawn from such a comparison.

1.2 Objective

An international collaboration of such magnitude will require a collection center to which all international representatives send their data. These data will be overlayed and plotted for comparison. Experts can then use these plots to make observations and comment on the different CFD codes used. With a collection site that is easily accessible to all parties involved and is set up to handle the enormous amount of data, the tasks of data processing and comparison will be quicker and carried out more efficiently.

The goal of this project is to assist WG-26 in collecting their predictions, plotting them against experimental data, and conducting an error analysis on the calculated results for comparison. This project will contribute to the final paper from the Working Group.

Chapter 2: Test Cases

2.1 Overview

To assess the credibility of results from CFD codes, a collection of standard test cases has been used by the aerospace industry and software developers as a quality assurance check before releasing their codes to users. These test cases have been selected to represent a wide range of CFD applications and modeling features. Due to time and effort constraints, the Working Group selected only two test cases for the validation exercise. The National Aeronautics and Space Administration (NASA) axial-flow compressor Rotor 37 and the Deutsche Forschungs- und Versuchsanstalt fuer Luft- und Raumfahrt (DLR, Germany) Turbine Stator were chosen as the two test cases for the Working Group. Representatives from NASA and DLR in the Working Group provided the experimental data necessary for comparison.

2.2 NASA Rotor 37 Test Case

Designated as NASA Stage 37, this test compressor is a low aspect ratio transonic core compressor inlet stage. This is a well-documented test case and has been used by many turbomachinery experts for comparison with CFD codes. For this reason, it is an ideal candidate for the Working Group's analysis. The experimental data and supporting literature of Rotor 37 was provided by Dr. Robert Delaney of Allison Engine Company, a member of the Working Group.

2.3 DLR Turbine Stator Test Case

A turbine test case was included in this exercise to demonstrate the capabilities required of a CFD code for use in turbomachinery design applications and its ability to predict key turbomachinery design characteristics.

The annular test cascade is a scaled version of a subsonic, low aspect ratio turbine stator. It is a frequently-used test case for the German aerospace industry, and its high quality experimental data and detailed geometry are readily available. Its Laser-Two-Focus-velocimeter (L2F) experimental data was provided by Dr. Henrich Weyer from DLR, who is a German authority in the turbomachinery field and a participant of the Working Group.

2.4 Working Group Members

The WG-26 consists of members from nations of the North Atlantic Treaty Organization (NATO) alliance. These members represent affiliations like Universities, aircraft engines manufacturers, governmental and other aerospace research establishments. The following table lists the investigators involved in this AGARD exercise.

Table 2.1: Investigators involved in the AGARD WG-26 exercise.

Investigator(s)	Affiliation	CFD Code Used	Test Cases
Robert Delaney and Scott McNulty	Allison Engine Co.	ADPAC	Both
Brad Hutchinson and Mihajlo Ivanovich	Advanced Scientific Computing Ltd. (ASC)	TASCflow	Rotor 37
John Calvert	Defence Research Agency (DRA)	DRA TRANSCode	Both
Stephan Lisiewicz	German Aerospace	TRACE_S	DLR
Francesco Bassi and Marco Savini	University of Bergamo	Bassi-Savini	DLR
Vincent Couaillier	ONERA	CANARI	Both
Andrea Dadone and Pietro De Palma	IME	Dadone-De Palma	DLR
Leonhard Fottner and Thomas Hildebrandt	Institut für Strahlantriebe (ISA)	TRACE_S & TASCflow	Rotor 37

The “Investigator(s)” column lists the names of the members in the Working Group and the “Affiliation” reflects the affiliation or organization they represent. “CFD Code Used” shows the lists of CFD codes the investigators will be using in this AGARD exercise to generate their results. Finally, “Test Cases” lists the test case data that the investigators have submitted. It should be noted that some investigators have submitted data for both test cases, as indicated in the “Test Cases” column. For example, results for both the DLR Turbine Stator and NASA Rotor 37 test cases were received from Dr. Robert Delaney and Scott McNulty of Allison Engine Company.

Chapter 3: Apparatus and Procedure

3.1 Overview

This section describes the means of collecting the predictions from investigating members of the Working Group and the methods used to compare the results from experimental data. Also discussed in this section are the tools and software used to plot the results.

3.2 Data Collection Methods

As internet access is widespread and convenient, it is conceived that the internet is the most efficient mean of collecting data from the Work Group. A computer equipped with an Ethernet card was reserved in the Turbomachinery laboratory at Virginia Tech to facilitate this cause. Using "QVT net" software, it was configured as a "file transfer protocol" (FTP) site which facilitated file transfer purposes. Investigators could log onto the computer through internet and "FTP" (a jargon for internet users) their data. As an alternate means for data collection, Work Group members could also send their data files in American Standard Characters II (ASCII) format to the author's Virginia Tech electronic mail (e-mail) account.

With these two internet locations in place, the Working Group was notified of the procedure to access and transfer files to these sites. Also members were advised to send their data files in ASCII, column-wise format. This is to facilitate the plotting effort of the investigating student using TECPLOT visualization software.

3.3 Data Visualization

Since visualization software was needed to present and compare WG-26 predictions and experimental data, TECPLOT version 6 was used as it is readily available in Turbolab. As TECPLOT requires data files to conform to a certain format, data sent by the Working Group members had to be manipulated to TECPLOT format. This tedious task of data manipulation was facilitated with the help of tools such as Microsoft Excel spreadsheet. The data files were imported into Excel and the data was manipulated with relative ease using “cut and paste” operations. Occasionally, small Fortran codes were written to manipulate large data files. A sample of the Fortran codes is listed in Appendix B.1.

The data files from all the investigators were not sorted uniformly. Some investigators arranged their data in a block of several columns, with the first column listing the dependent variables and the subsequent columns listing the independent results. Other investigators preferred to arrange their data in a one-to-one format; one column of independent variable with the corresponding column listing the independent results. To conveniently plot them in TECPLOT, files of data were arranged into dual-column, x-y axes type format with the first column being the dependent values (usually the percentage span or height of blade) while the calculated data (e.g. total pressure ratio) in the other column. Sets of data with the same axes were then sorted and labeled as zones. These zones represented different investigators, grids or turbulence models and allowed TECPLOT to distinguish different sets of data in a file. The user could also change the attributes associated to these zones on the plots in TECPLOT.

A sample of the TECPLOT data file that was used to generate the spanwise overall pressure ratio plot in Figure 4.1 is listed in Appendix B.2. The different sets of data sent by different investigators were listed in one file and their plots were superimposed on the experimental data to create a color plot for comparison. As TECPLOT uses zones to distinguish different sets of data, each zone in the data files represents either different investigators, grids or turbulence models. Detailed descriptions of the representation of the zones are listed in the legend of the figure.

Once these data files were prepared, TECPLOT automatically converted the files into binary data files to generate the plots. Copies of these plots were sent to the respective investigators for validation. The investigators were asked to review the plots to verify that the plots were exact representation of their data.

3.4 Error Analysis

The error analysis for this project is not an attempt to account for the error in the experimental data but is the actual deviation of the investigators' results from the experimental data. The experimental data is assumed to be an accurate representation of the test cases.

3.4.1 Collecting Data for Error Analysis

As different investigators used different increments for their independent parameters, it was not possible to make a comparable calculation of the deviation between experimental and predicted results. To bridge this problem, TECPLOT has a interpolation feature that will linearly interpolate values between points on a graph. All

that is required of the user is to specify the independent coordinates of the experimental values and TECPLOT will interpolate the graphs of the predicted values. The only drawback is that TECPLOT does not store the lists of results. To overcome this, the user must key in the points and register the output one at a time.

With this interpolation feature, the experimental data points were keyed into TECPLOT to linearly interpolate between points across the investigators' graphs to yield the corresponding data points. For example, the first experimental data point for Figure 4.3 is at 5% of the span and the value 2.1196 on the Total Pressure Ratio axis. TECPLOT will then interpolate between points on the ADPAC curve to return a value of 2.2559. This indicates that at 5% span, the ADPAC code should yield a Total Pressure Ratio of 2.2559 according to linear interpolation. Thus, the subsequent points on the TASCflow, DRA TRANScode, CANARI, and other curves at 5% span were interpolated and recorded. These data points were tabulated in a Microsoft Excel spreadsheet and similar tables were generated for Figures 4.1 through 4.10 in Chapter 4. The results are tabulated in Tables C.1 through C.10 in Appendix C. The author can conduct error analyses based on these tables.

3.4.2 Method of Analysis

Absolute error of the predictions (deviation) are evaluated by subtracting the local value of the best-fit curve from the experimental value. The largest error of the list is recorded as the maximum deviation. Therefore, deviation is defined as:

$$\delta_i = |x_i - y_i| \quad (1)$$

where δ represents deviation, x represents the experimental data, and y represents the calculated data points. The subscript, “ i ”, indicates the corresponding pairs of the experimental and calculated data. This form of representation for the deviation, experimental data and its corresponding calculated data will be consistent throughout this section.

Several methods are used in this project to analyze the error. These methods are commonly used in engineering as preliminary evaluation of data. The first method involves finding the maximum deviation. This is computed using the expression:

$$\delta_{\max} = \max \left| \left(x_1 - y_1 \right), \left(x_2 - y_2 \right), \left(x_3 - y_3 \right), \dots, \left(x_n - y_n \right) \right| \quad (2)$$

The second method involves evaluating the mean deviation

$$\delta_{\text{mean}} = \frac{\sum |x_i - y_i|}{N} \quad (3)$$

where N in the denominator represents the total number of data points.

This method simply computes the average of all the deviation values of each investigator.

Next, the root-mean-square (rms) deviation can be evaluated using the expression:

$$\delta_{\text{rms}} = \sqrt{\frac{\sum (x_i - y_i)^2}{N}} \quad (4)$$

The percentage deviation is simply the ratio of the deviation (described in Equation 1) and the corresponding experimental data point.

$$\delta_i(\%) = \frac{|x_i - y_i|}{x_i} \times 100\% \quad (5)$$

The maximum percentage deviation is the maximum of the percentage deviation described in Equation 5.

$$\delta_{\max}(\%) = \max \left| \frac{(x_1 - y_1)}{x_1}, \frac{(x_2 - y_2)}{x_2}, \frac{(x_3 - y_3)}{x_3}, \dots, \frac{(x_n - y_n)}{x_n} \right| \times 100\% \quad (6)$$

The mean percentage deviation is the mean of the percentage deviation.

$$\delta_{\text{mean}}(\%) = \frac{1}{N} \sum \left[\frac{|x_i - y_i|}{x_i} \times 100\% \right] \quad (7)$$

Finally, the rms percentage deviation is defined as:

$$\delta_{\text{rms}}(\%) = \sqrt{\frac{\sum \left(\frac{(x_i - y_i)}{x_i} \times 100\% \right)^2}{N}} \quad (8)$$

With these equations defined, the results are plotted in Figures 4.11 through 4.30 in Chapter 4.

Chapter 4: Results

4.1 Types of Results

Four different types of results are shown in this section. The overplots of the predicted data and experimental values for NASA Rotor 37 test case, the DLR Turbine Stator test case, the bar charts showing the error analysis of the NASA Rotor 37, and the bar charts reflecting the error analysis for the DLR Turbine Stator test case are presented.

Various colors and symbols are used to distinguish between investigators in the overplots (Figures 4.1 through 4.10). To distinguish investigators with more than one set of data, different symbols of the same color are used to represent their data. For example, blue hollow circles and squares are used to distinguish the two grids used by Lisiewicz in his TRACE_S results for the DLR Turbine Stator Test Case (Figures 4.6 through 4.10). Note that black, solid diamonds represent the experimental data for all the overplots.

Figures 4.11 through 4.30 show the bar charts for the results of the error analyses using equations 2 through 7. As the names in the legend suggest, the maximum deviation ("Max Deviation") lists the results from using Equation 2 (Section 3.4.2, pp. 9), mean deviation ("Mean Deviation") from Equation 3, and root-mean-square deviation ("Rms Deviation") from Equation 4. The maximum percentage deviation ("Max Percentage Deviation"), mean percentage deviation ("Mean Percentage Deviation") and root-mean-square percentage deviation ("Rms Percentage Deviation") values are the results from computations using Equations 6, 7 and 8, respectively.

4.2 Results for the NASA Rotor 37 Test Case

Figures 4.1 through 4.5 show the overplots for the predicted results from five investigators (Table 2.1). Figure 4.1 reflects the results for the overall pressure ratio, and Figure 4.2 shows the overall efficiency. Figure 4.3 shows the spanwise distribution of the total pressure ratio data, Figure 4.4 shows the spanwise distribution of the total temperature ratio values and Figure 4.5 shows the spanwise distribution of adiabatic efficiency. It should be noted that Fottner and Hildebrandt used TASCflow and TRACE_S for their predictions, and that these were the same codes used by Hutchinson and Ivanovich, and Lisiewicz respectively. To differentiate the three investigators' results, "X" symbols are used to show the results from Fottner and Hildebrandt. This is clearly noted in the legend as "TASCflow (F&H) Prediction" and "TRACE S (F&H) Prediction."

Figure 4.1: NASA Rotor 37 Test Case
Overall Pressure Ratio vs. Normalized Mass Flow

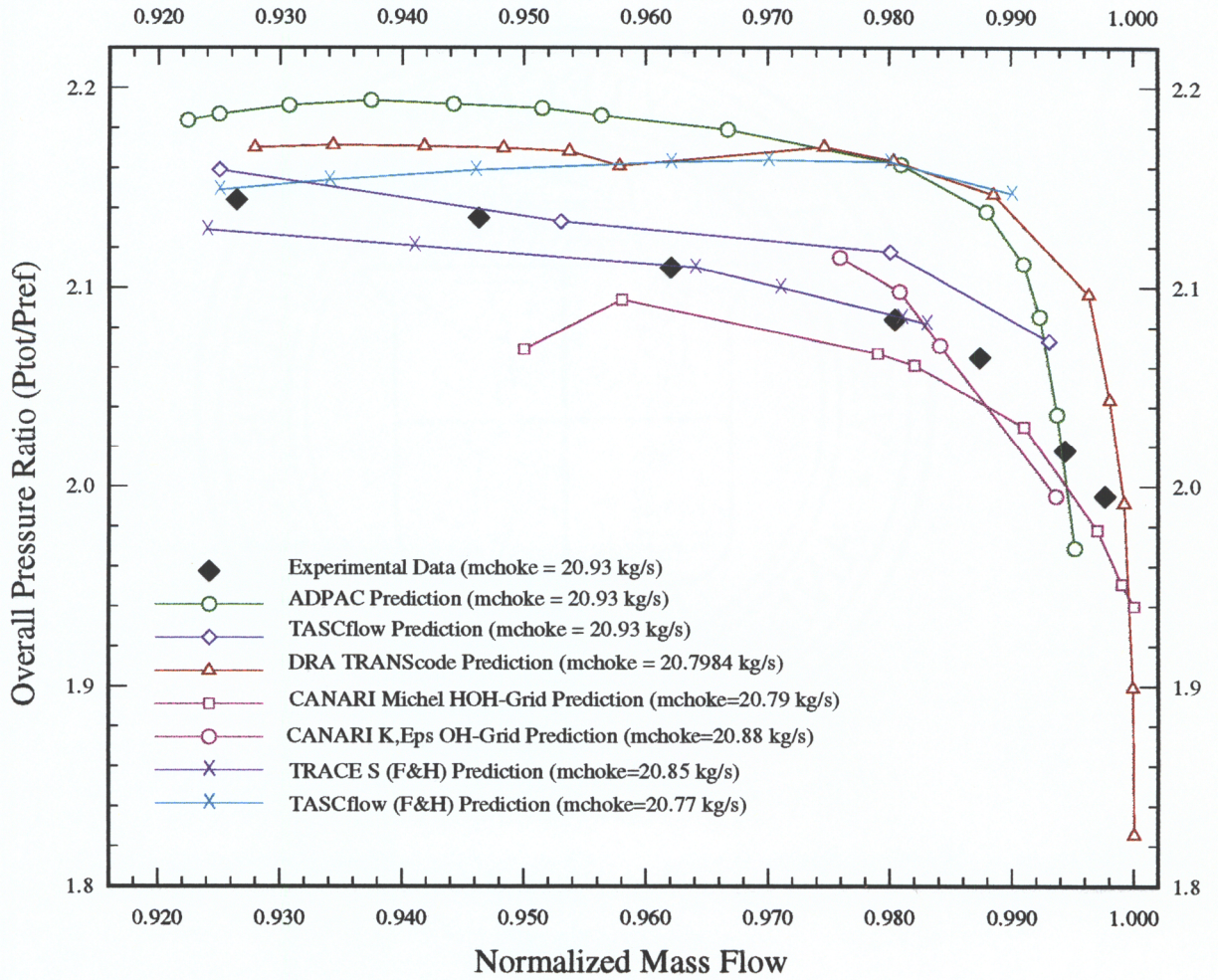


Figure 4.2: NASA Rotor 37 Test Case
Overall Efficiency vs. Normalized Mass Flow

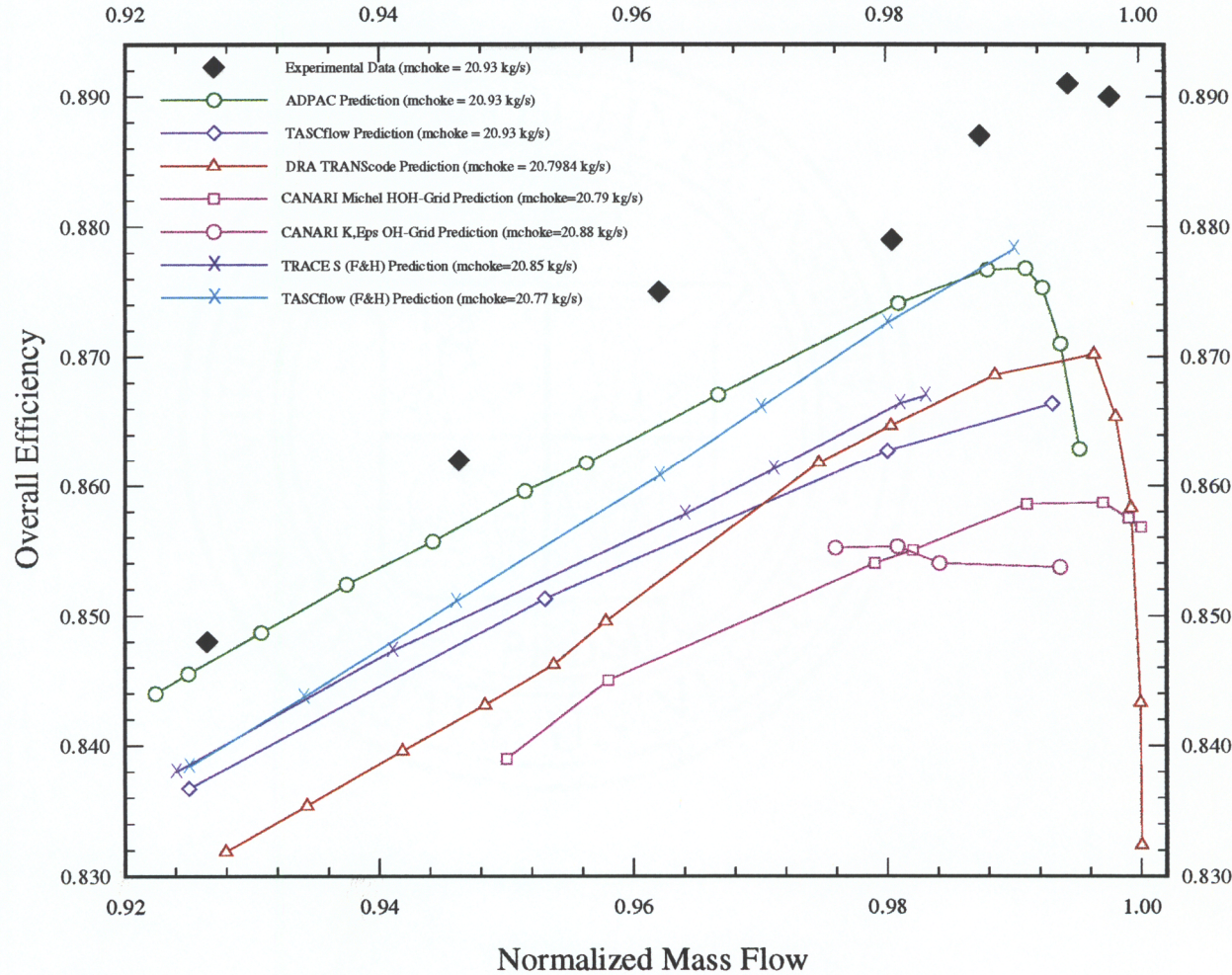


Figure 4.3: NASA Rotor 37 Test Case
Spanwise Distribution of Total Pressure

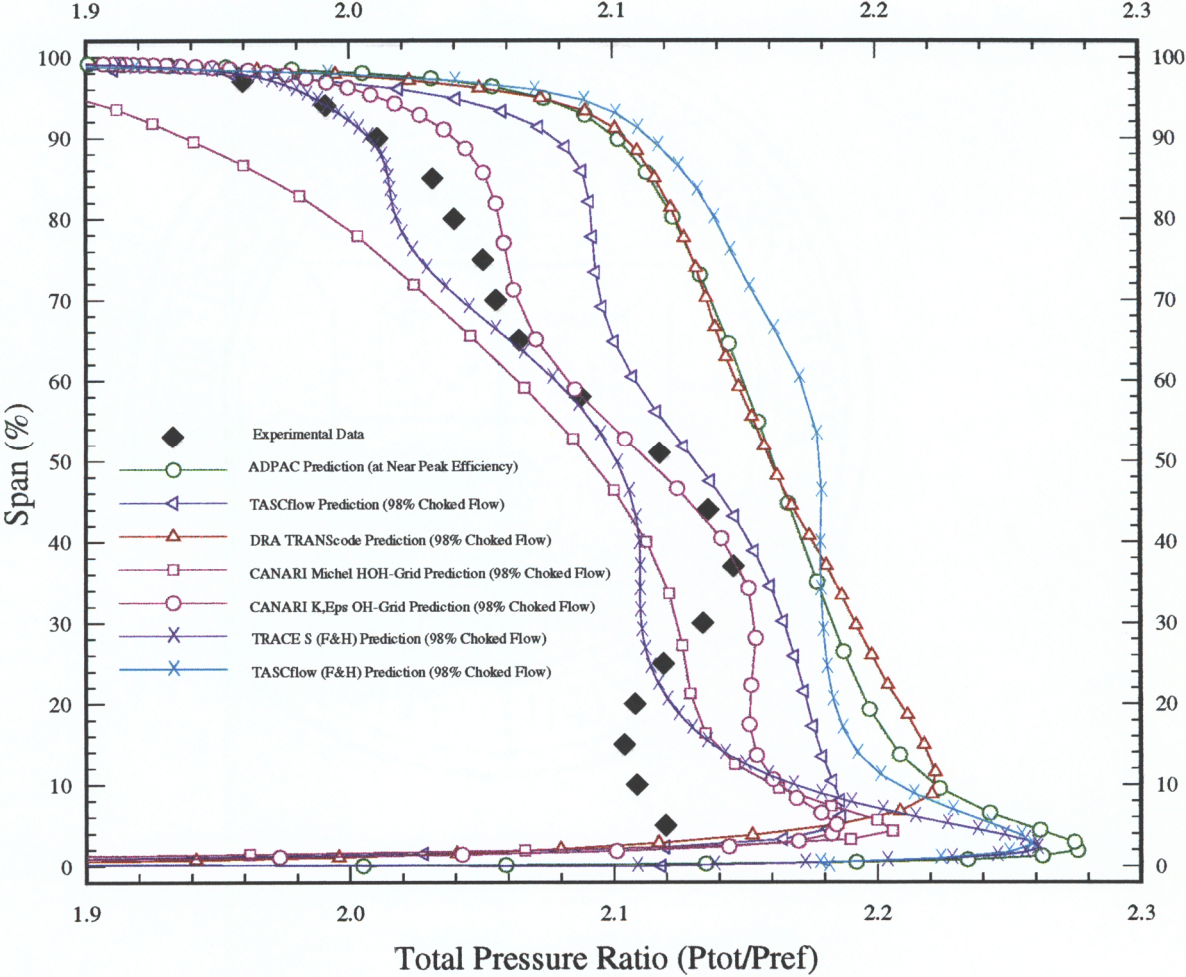


Figure 4.4: NASA Rotor 37 Test Case
Spanwise Distribution of Total Temperature

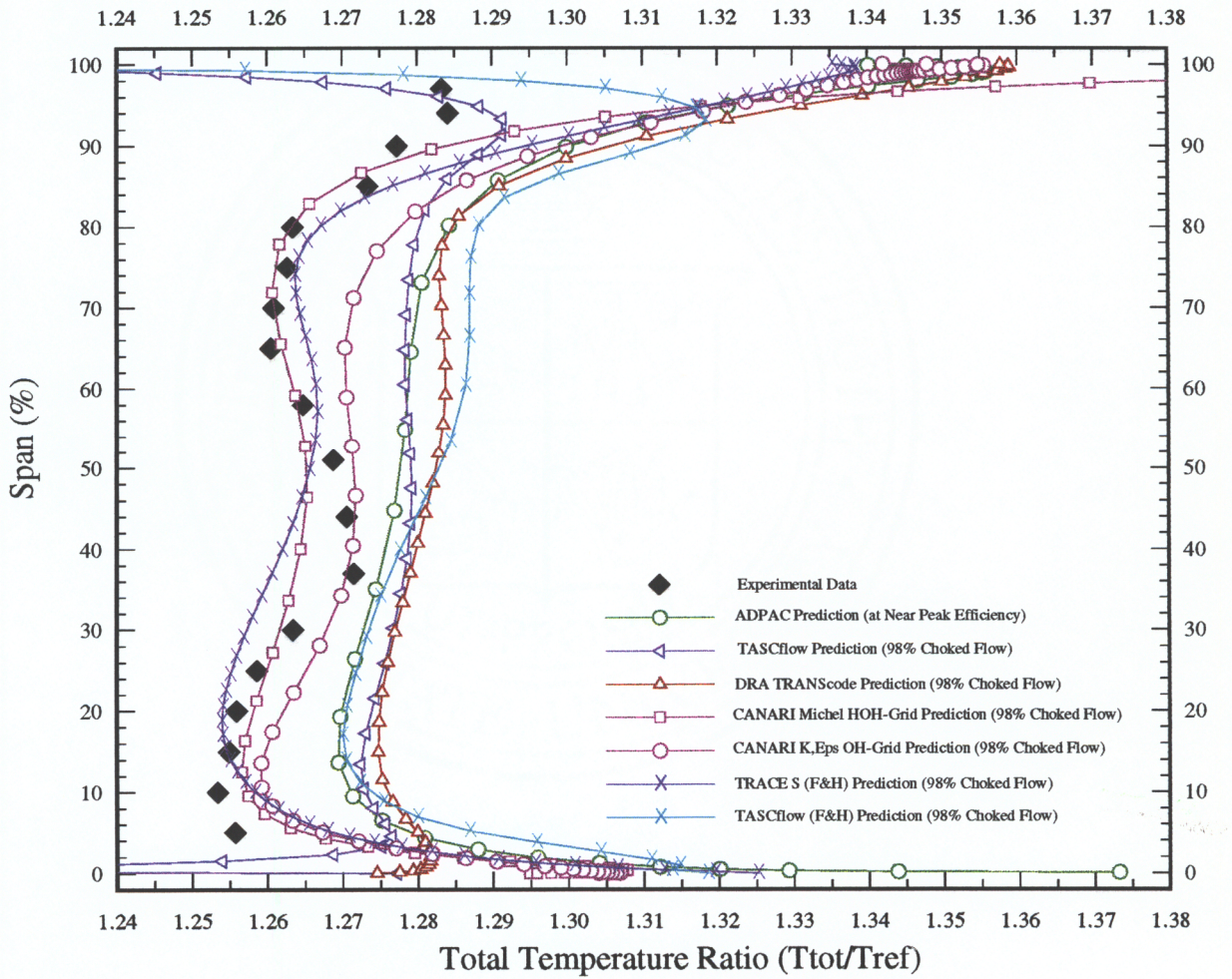
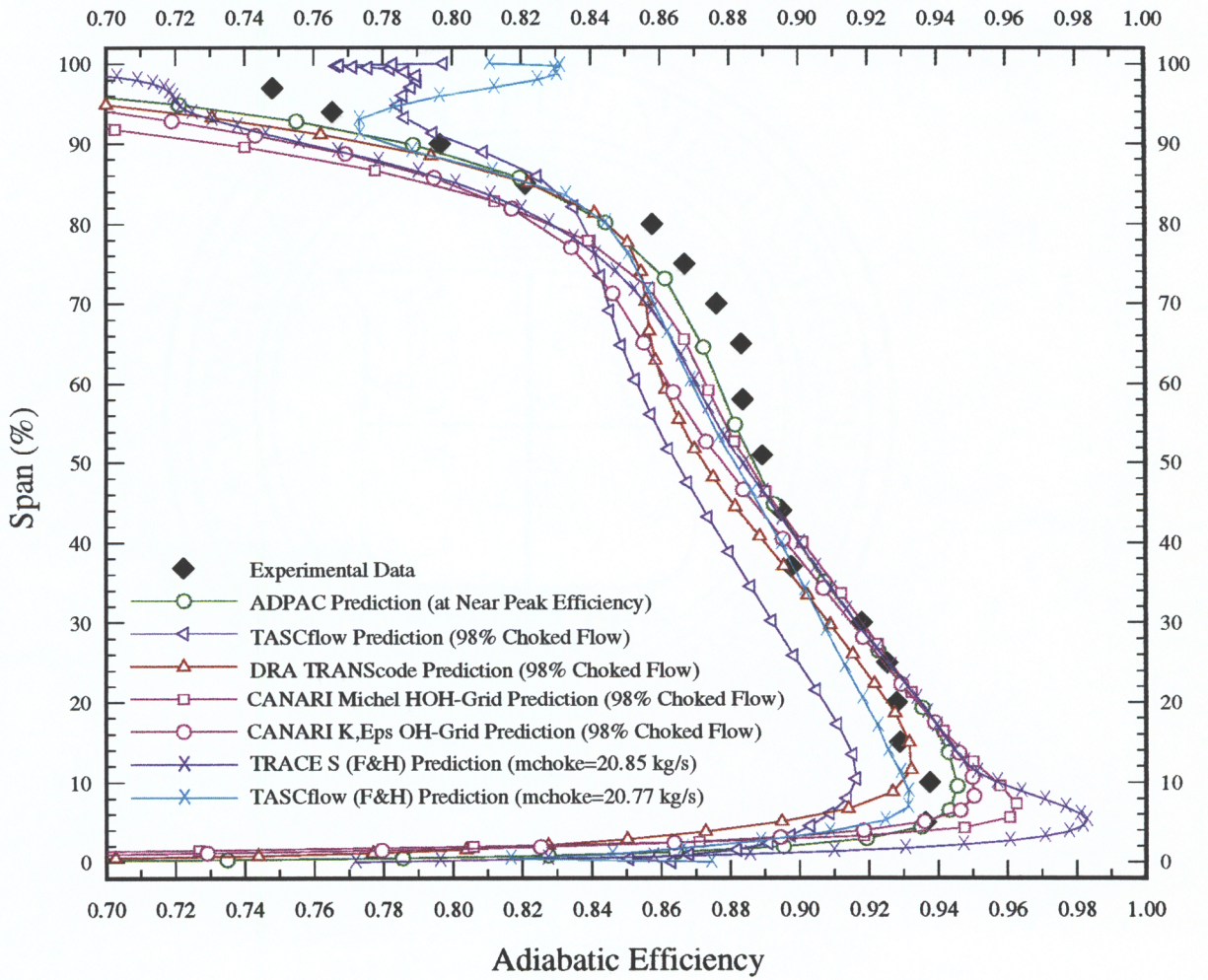


Figure 4.5: NASA Rotor 37 Test Case
Spanwise Distribution of Adiabatic Efficiency



4.3 Results for the DLR Turbine Stator Test Case

Figures 4.6 through 4.10 show the overplots of the predicted results for the DLR Turbine Stator Test Case from six investigators (Table 2.1). Figures 4.6 and 4.6a reflect the pitchwise averaged exit circumferential flow angles (Figure A.2 in Appendix A) at station X/C_x of 1.40, which is located at the exit of the DLR turbine stator flow passage. Since the results from the investigators are too close to be plotted in one figure, the results are divided into two plots. Figure 4.6 lists results from Calvert, Lisiewicz, and Bassi and Savini while Figure 4.6a lists predictions from Couaillier, and Delaney and McNulty.

Figure 4.7 plots the pitchwise averaged exit radial flow angles (Figure A.1), Figure 4.8 shows the pitchwise averaged exit mach number of the flow, and Figure 4.9 shows the pitchwise averaged of the static pressure ratio. Finally, Figure 4.10 compares the pitchwise averaged total pressure ratio predictions. Note that Figures 4.6, 4.6a and 4.7 do not list results from Dadone and De-Palma because these data had not been received from them at the time of this report.

Figure 4.6: DLR Turbine Stator Test Case
Pitchwise Averaged Exit Circumferential Flow Angles at $X/C_x=1.40$

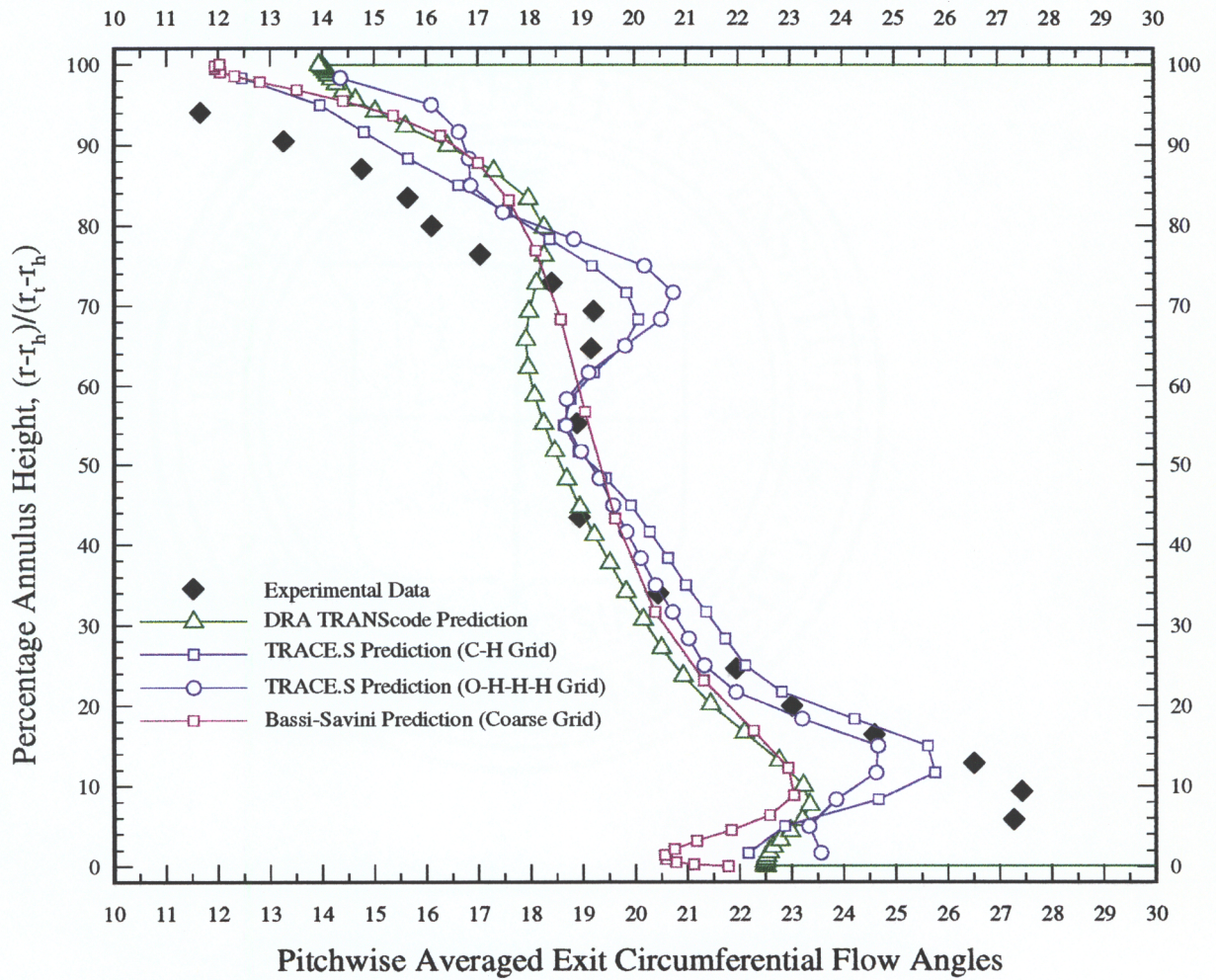


Figure 4.6a: DLR Turbine Stator Test Case

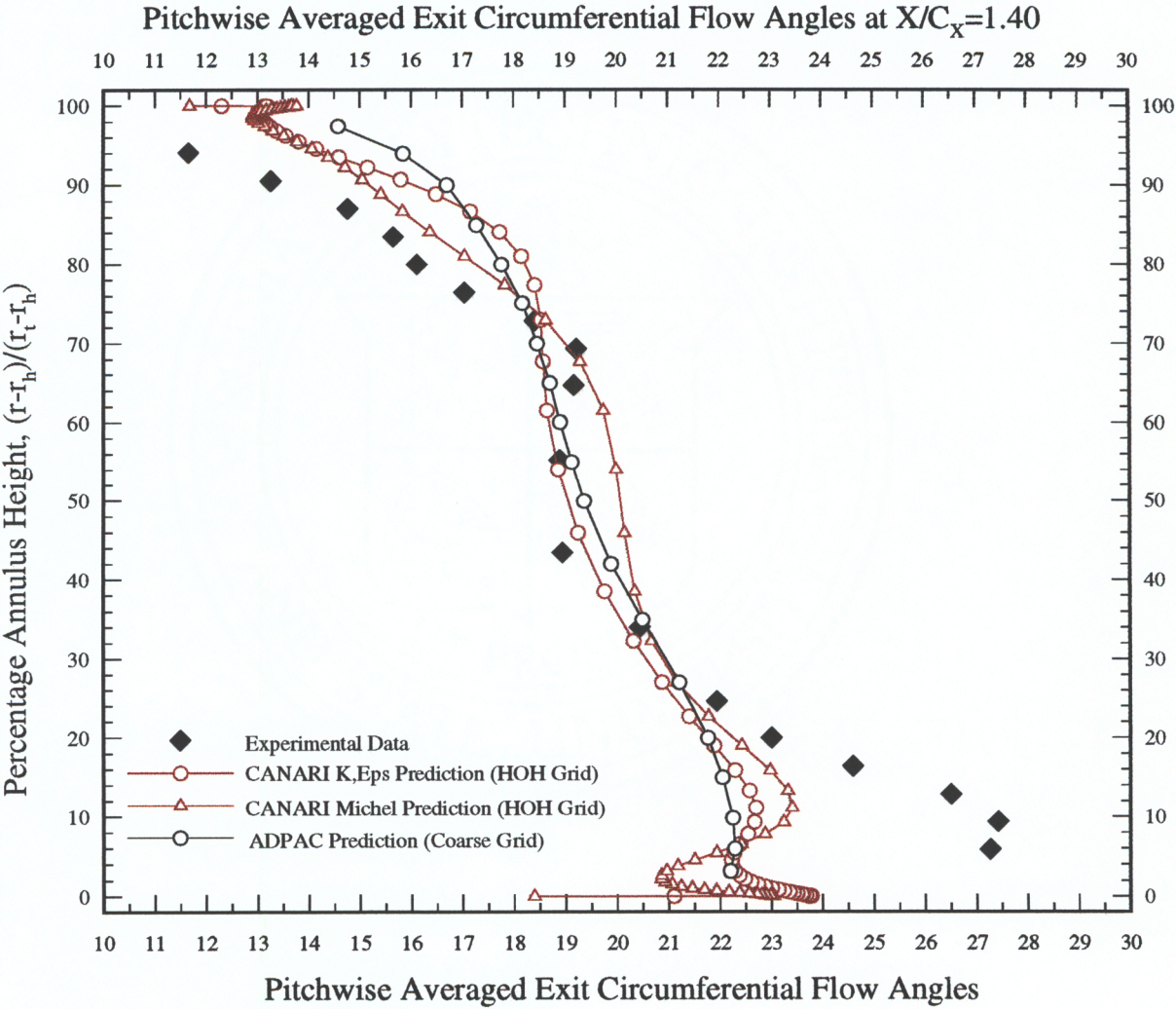


Figure 4.7: DLR Turbine Stator Test Case
Pitchwise Averaged Exit Radial Flow Angles at $X/C_x=1.40$

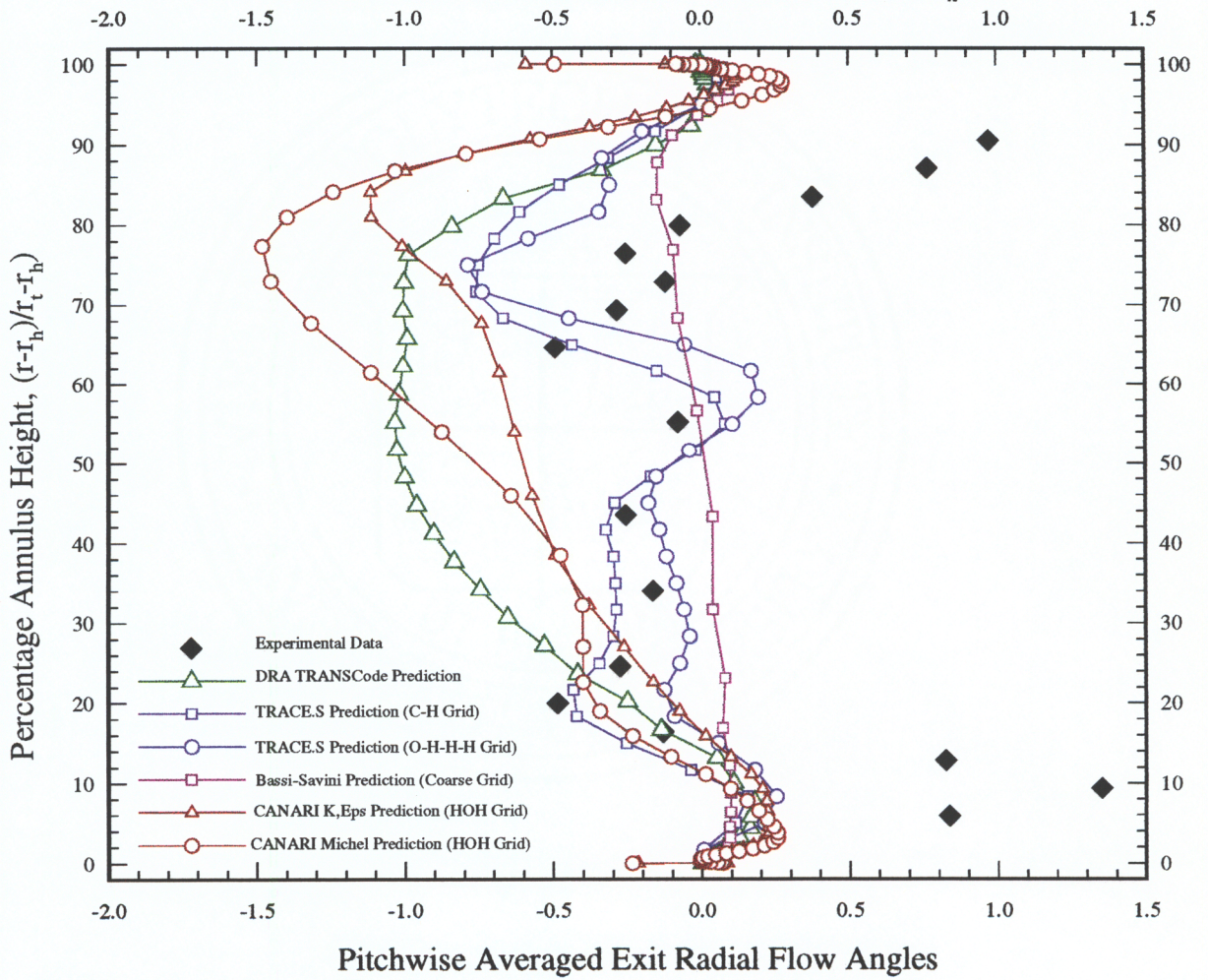


Figure 4.8: DLR Turbine Stator Test Case
Pitchwise Averaged Exit Mach Number at $X/C_x=1.40$

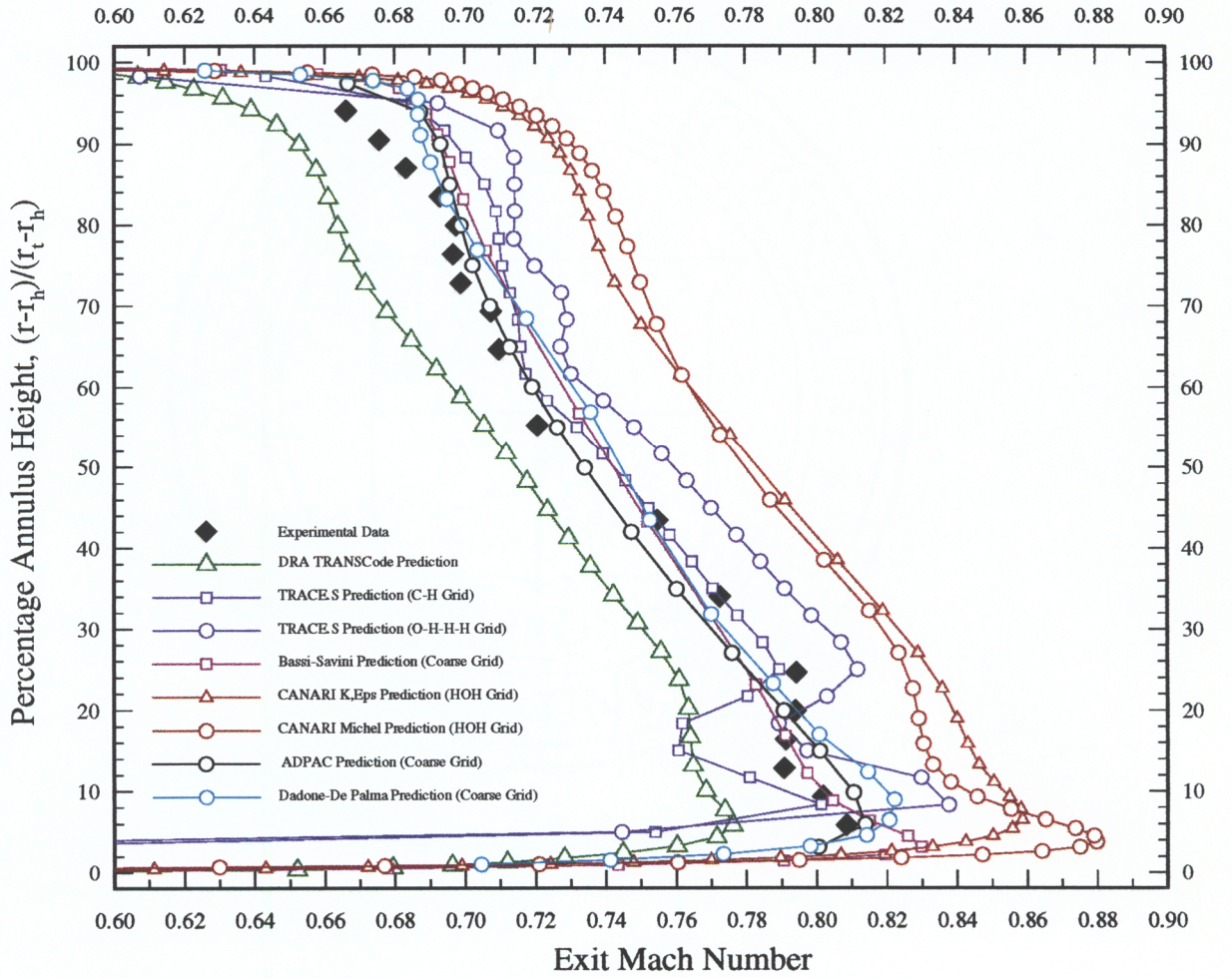


Figure 4.9: DLR Turbine Stator Test Case

Pitchwise Averaged P_s / P_{o1} at $X/C_x=1.4$

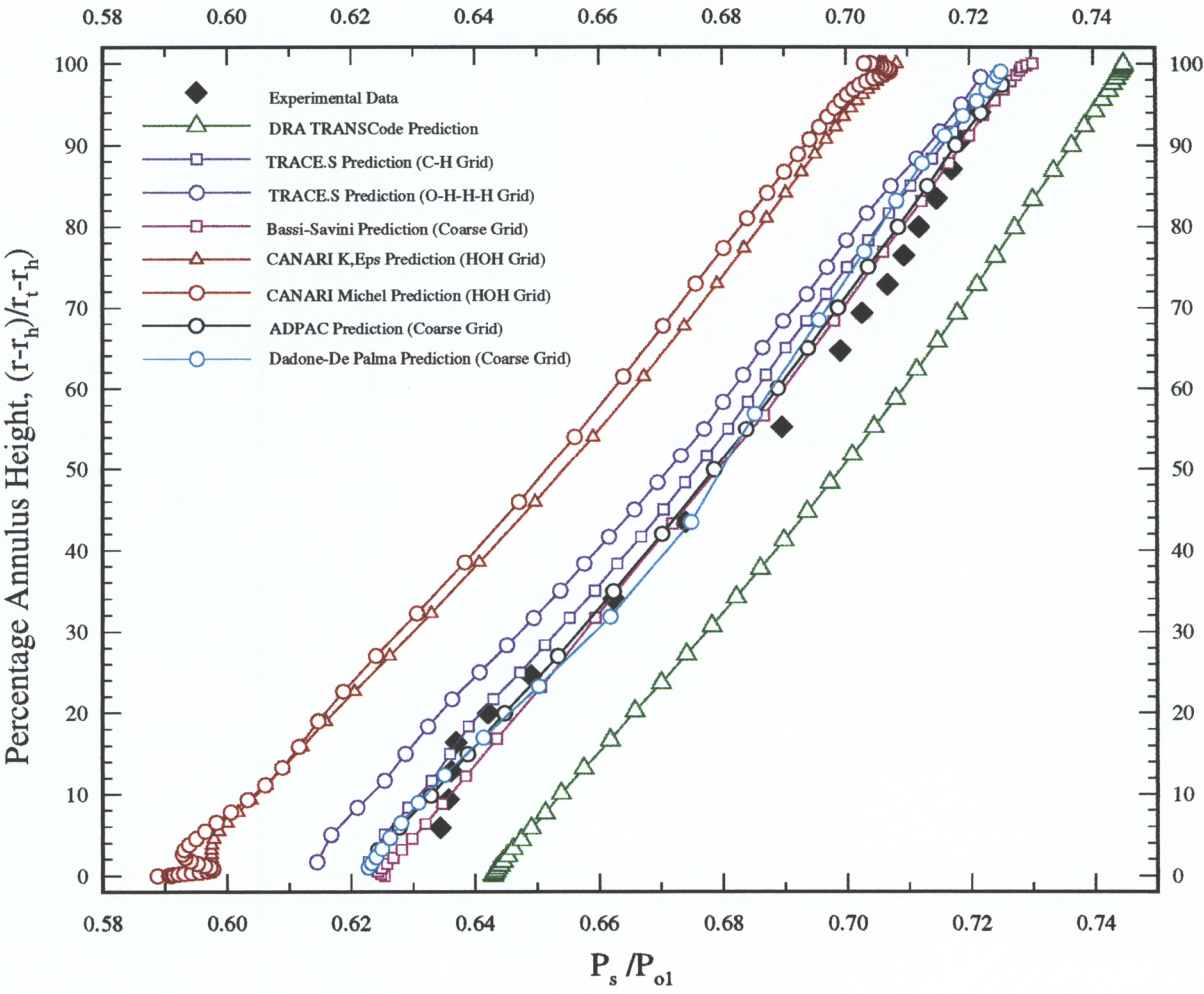
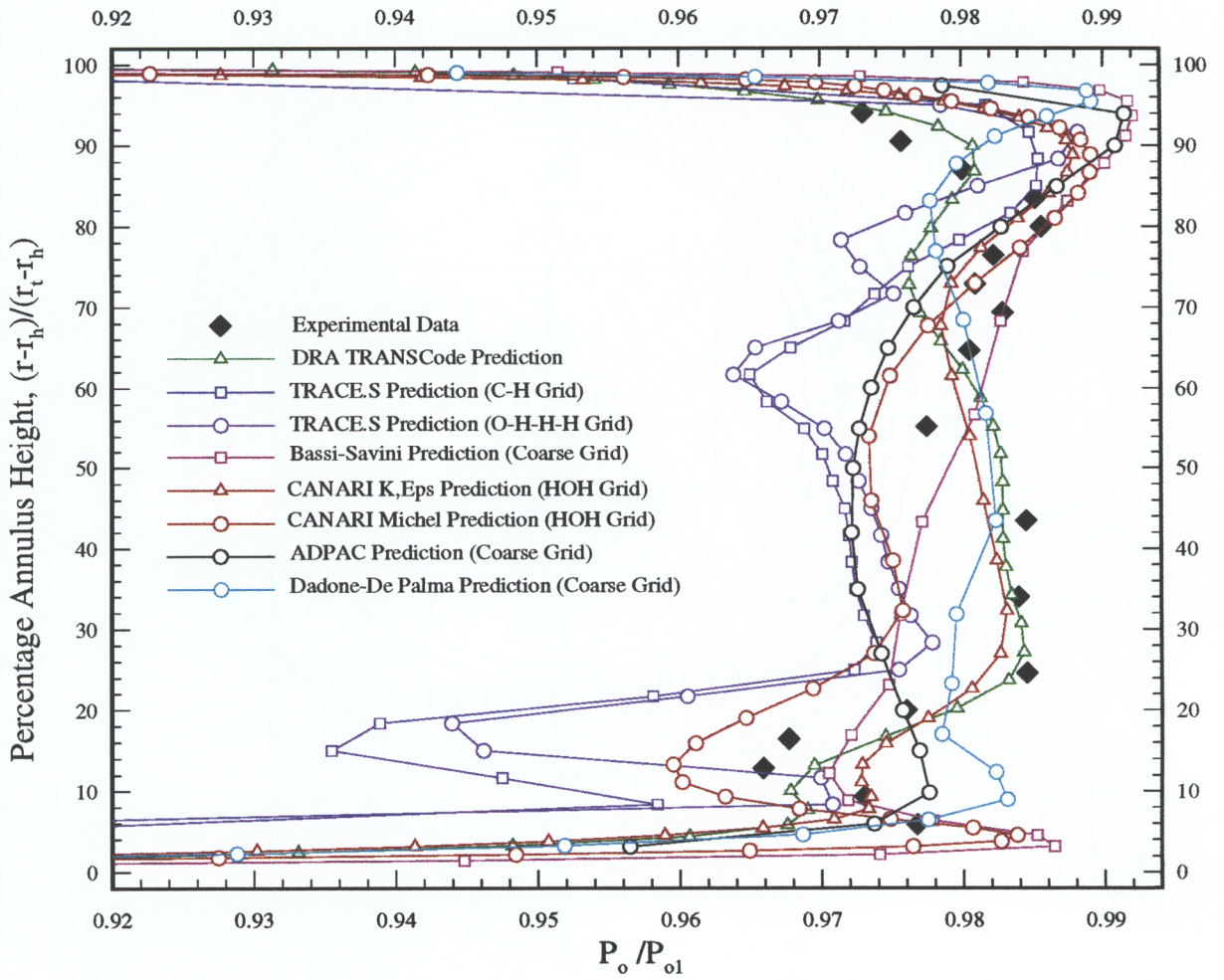


Figure 4.10: DLR Turbine Stator Test Case
Pitchwise Averaged P_o/P_{o1} at $X/C_x=1.4$

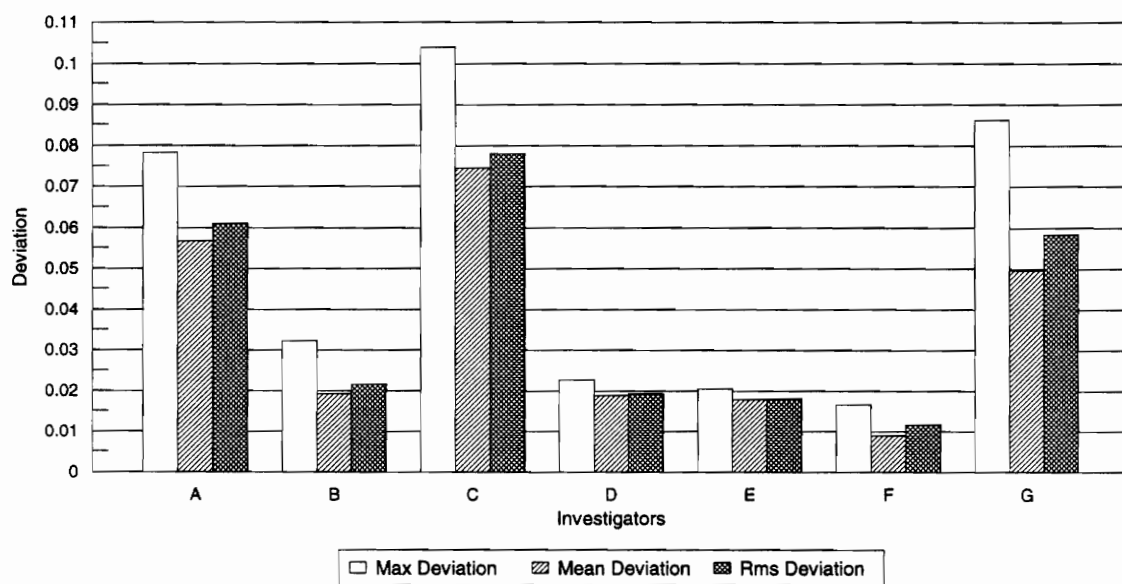


4.4 Results from the Error Analysis

Figures 4.11 through 4.30 show the results from the error analysis described in Section 3.4.2. These bar charts reflect the error analysis of the data in Figures 4.11 through 4.20. Figure 4.11 shows the difference (deviation) between the experimental and predicted values in Figure 4.1. Figure 4.12 shows the error (percentage deviation) of the data in Figure 4.1. Similarly, Figures 4.13 and 4.14 show the results of the error analyses for Figure 4.2 and the comparisons follow through to Figure 4.20. The titles for each figure are self-explanatory and they correspond to the figures from which the data are utilized for the error analysis.

Figure 4.11: NASA Rotor 37 Test Case

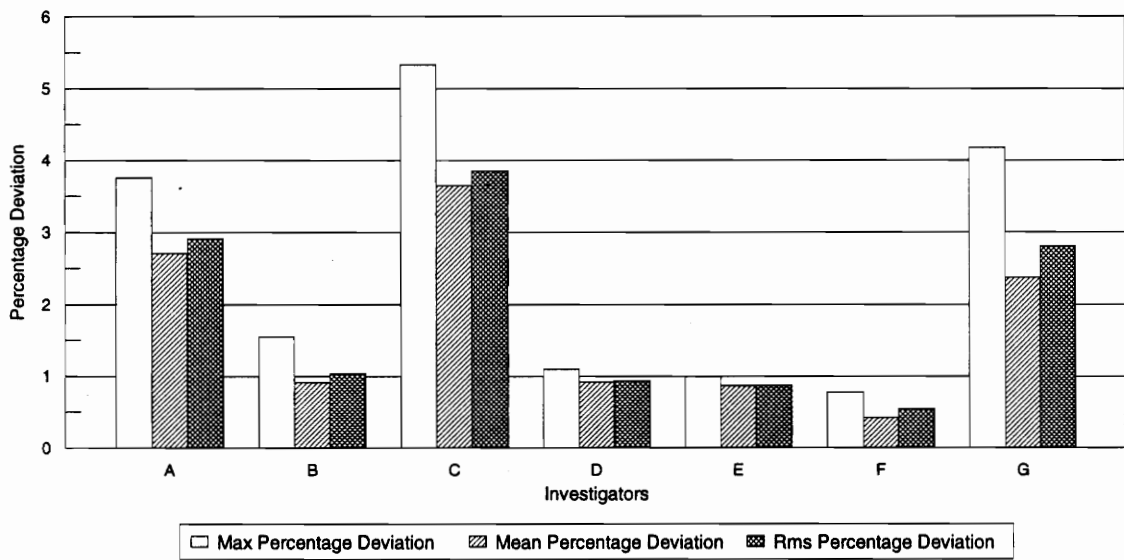
Difference (Deviation) between experimental and predicted values for Overall Pressure Ratio vs. Normalized Mass Flow Data



Notations for X-Axis: A = ADPAC, B = TASCflow, C = TRANSCode, D = CANARI (Michel) HOH-Grid, E = CANARI (K, Eps), F = Fottner/Hildebrandt TRACE_S, G = Fottner/Hildebrandt TASCflow

Figure 4.12: NASA Rotor 37 Test Case

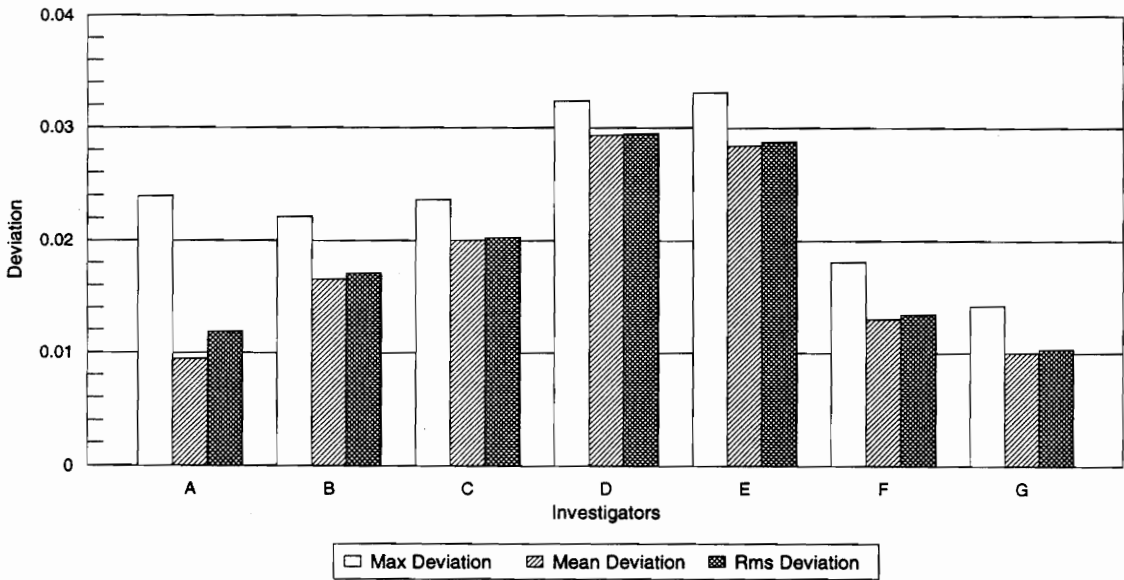
Percentage Difference (Deviation) between experimental and predicted values for Overall Pressure Ratio vs. Normalized Mass Flow Data



Notations for X-Axis: A = ADPAC, B = TASCflow, C = TRANSCode, D = CANARI (Michel) HOH-Grid, E = CANARI (K, Eps), F = Fottner/Hildebrandt TRACE_S, G = Fottner/Hildebrandt TASCflow

Figure 4.13: NASA Rotor 37 Test Case

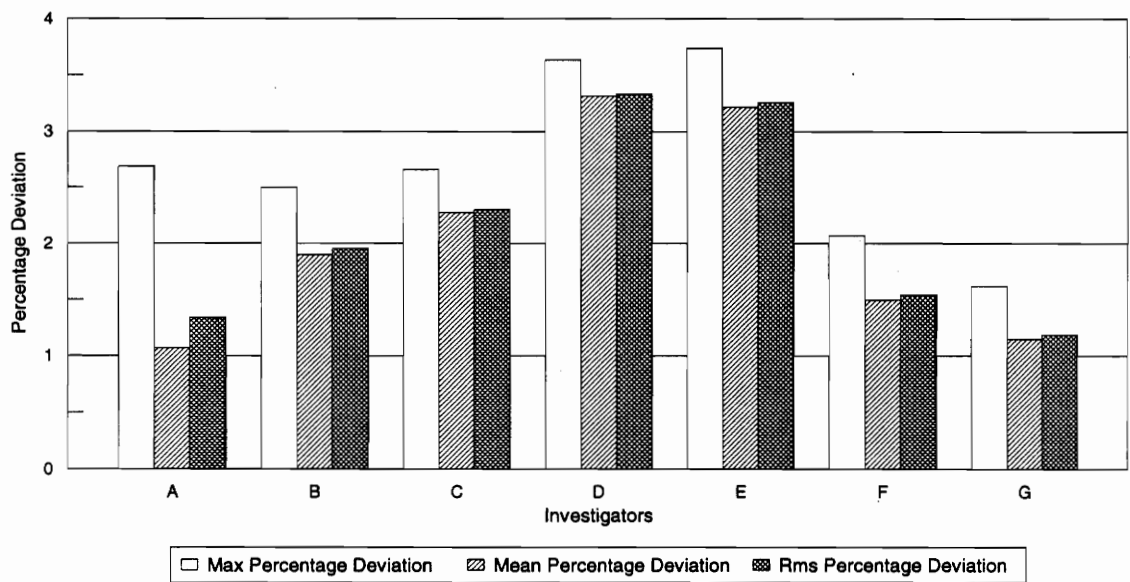
Difference (Deviation) between experimental and predicted values for Overall Efficiency vs. Normalized Mass Flow Data



Notations for X-Axis: A = ADPAC, B = TASCflow, C = TRANSCode, D = CANARI (Michel) HOH-Grid, E = CANARI (K, Eps), F = Fottner/Hildebrandt TRACE_S, G = Fottner/Hildebrandt TASCflow

Figure 4.14: NASA Rotor 37 Test Case

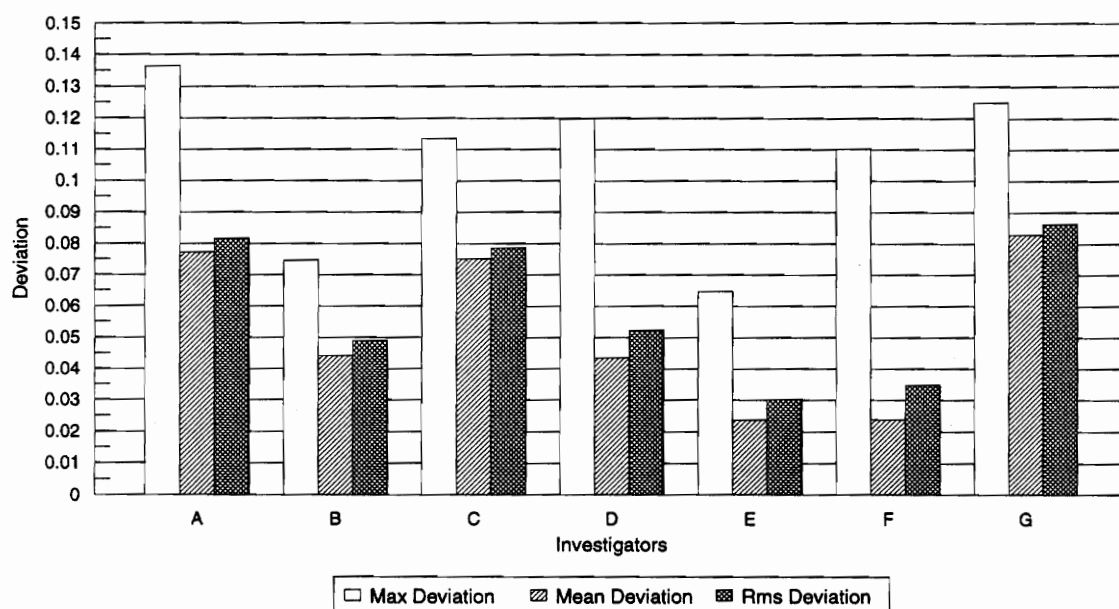
Percentage Difference (Deviation) between experimental and predicted values for Overall Efficiency vs. Normalized Mass Flow Data



Notations for X-Axis: A = ADPAC, B = TASCflow, C = TRANSCode, D = CANARI (Michel) HOH-Grid, E = CANARI (K, Eps), F = Fottner/Hildebrandt TRACE_S, G = Fottner/Hildebrandt TASCflow

Figure 4.15: NASA Rotor 37 Test Case

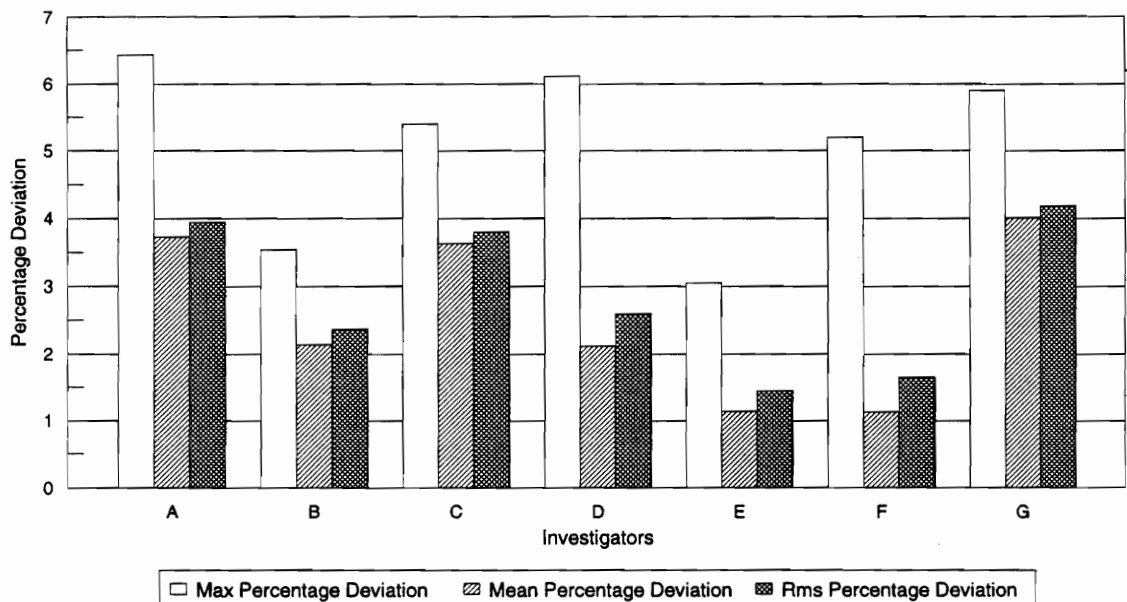
Difference (Deviation) between experimental and predicted values for Spanwise Distribution of Total Pressure Data



Notations for X-Axis: A = ADPAC, B = TASCflow, C = TRANSCode, D = CANARI (Michel) HOH-Grid, E = CANARI (K, Eps), F = Fottner/Hildebrandt TRACE_S, G = Fottner/Hildebrandt TASCflow

Figure 4.16: NASA Rotor 37 Test Case

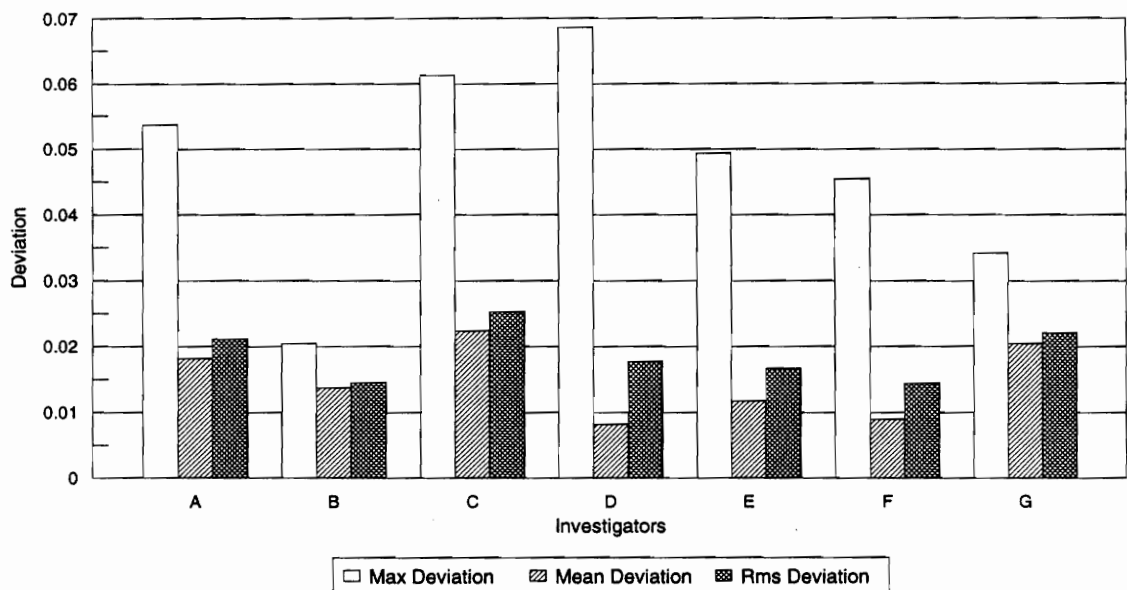
Percentage Difference (Deviation) between experimental and predicted values for Spanwise Distribution of Total Pressure Data



Notations for X-Axis: A = ADPAC, B = TASCflow, C = TRANSCode, D = CANARI (Michel) HOH-Grid, E = CANARI (K, Eps), F = Fottner/Hildebrandt TRACE_S, G = Fottner/Hildebrandt TASCflow

Figure 4.17: NASA Rotor 37 Test Case

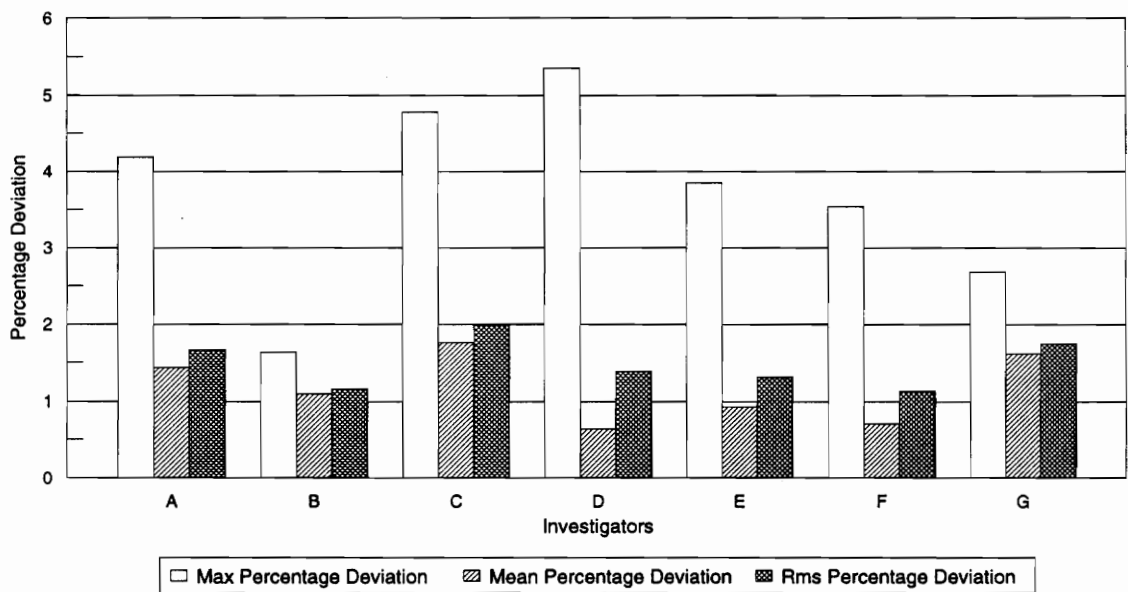
Difference (Deviation) between experimental and predicted values for Spanwise Distribution of Total Temperature Data



Notations for X-Axis: A = ADPAC, B = TASCflow, C = TRANSCode, D = CANARI (Michel) HOH-Grid, E = CANARI (K, Eps), F = Fottner/Hildebrandt TRACE_S, G = Fottner/Hildebrandt TASCflow

Figure 4.18: NASA Rotor 37 Test Case

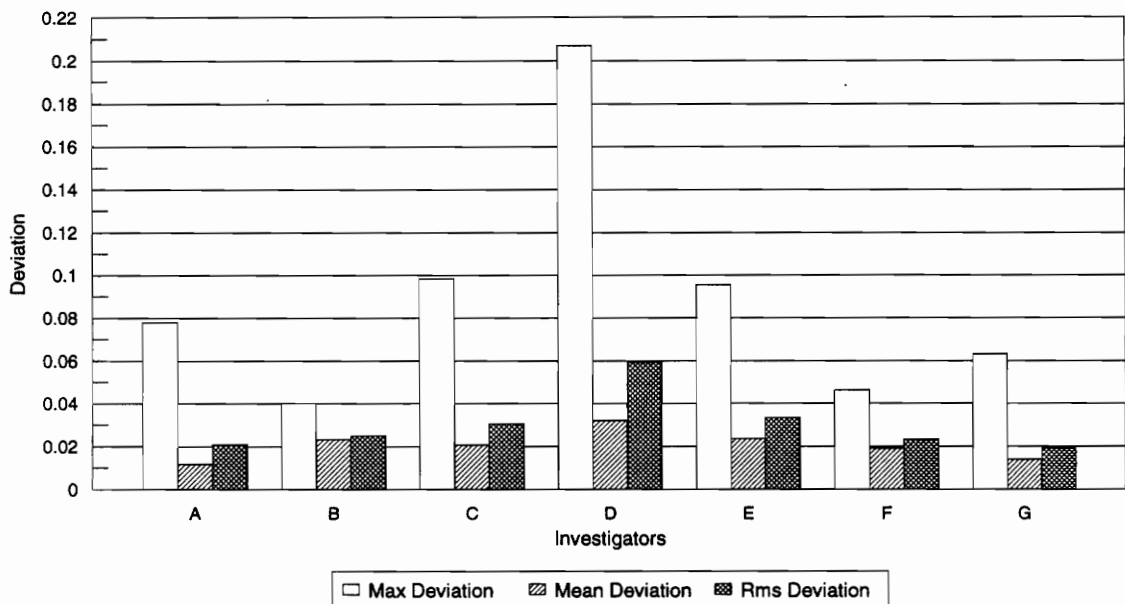
Percentage Difference (Deviation) between experimental and predicted values for Spanwise Distribution of Total Temperature Data



Notations for X-Axis: A = ADPAC, B = TASCflow, C = TRANSCode, D = CANARI (Michel) HOH-Grid, E= CANARI (Michel) OH-Grid, F = CANARI (K, Eps), G = Fottner/Hildebrandt TRACE_S, H = Fottner/Hildebrandt TASCflow

Figure 4.19: NASA Rotor 37 Test Case

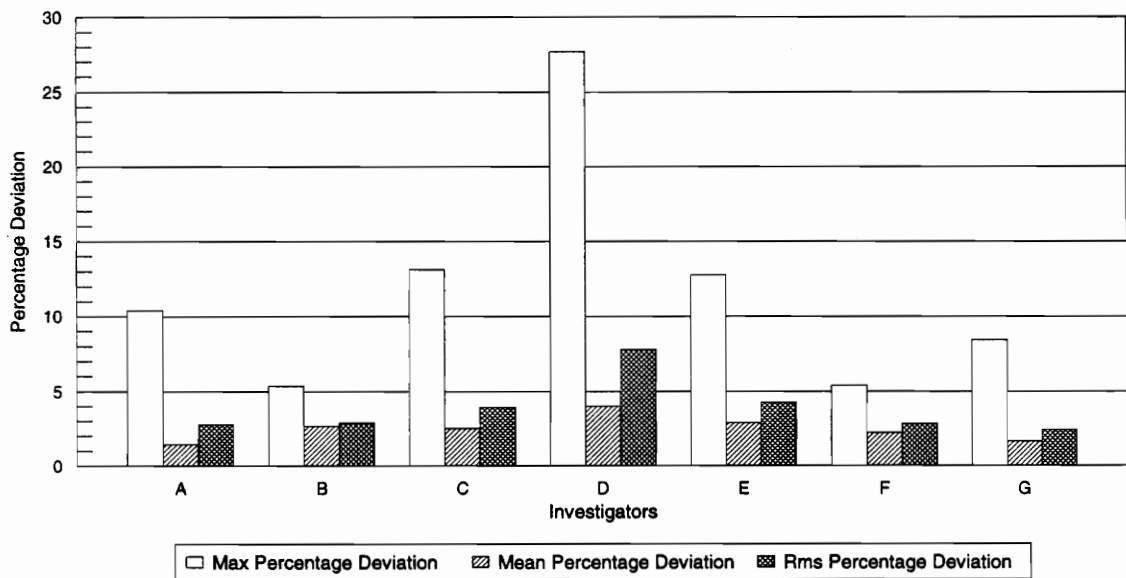
Difference (Deviation) between experimental and predicted values for Spanwise Distribution of Adiabatic Efficiency Data



Notations for X-Axis: A = ADPAC, B = TASCflow, C = TRANSCode, D = CANARI (Michel) HOH-Grid, E = CANARI (K, Eps), F = Fottner/Hildebrandt TRACE_S, G = Fottner/Hildebrandt TASCflow

Figure 4.20: NASA Rotor 37 Test Case

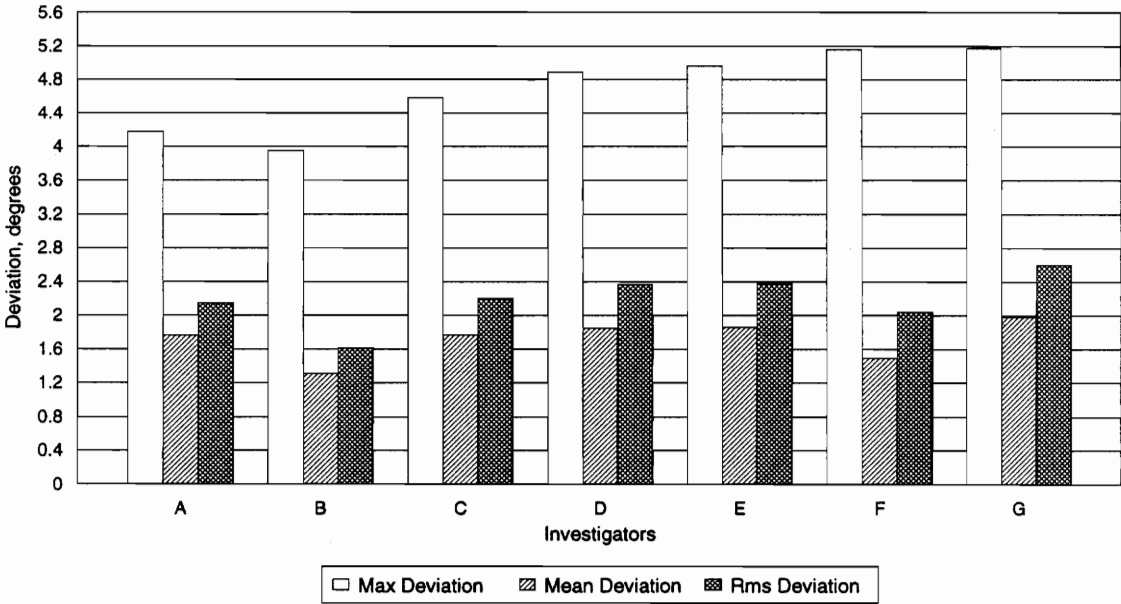
Percentage Difference (Deviation) between experimental and predicted values for Spanwise Distribution of Adiabatic Efficiency Data



Notations for X-Axis: A = ADPAC, B = TASCflow, C = TRANSCode, D = CANARI (Michel) HOH-Grid, E = CANARI (K, Eps), F = Fottner/Hildebrandt TRACE_S, G = Fottner/Hildebrandt TASCflow

Figure 4.21: DLR Turbine Stator Test Case

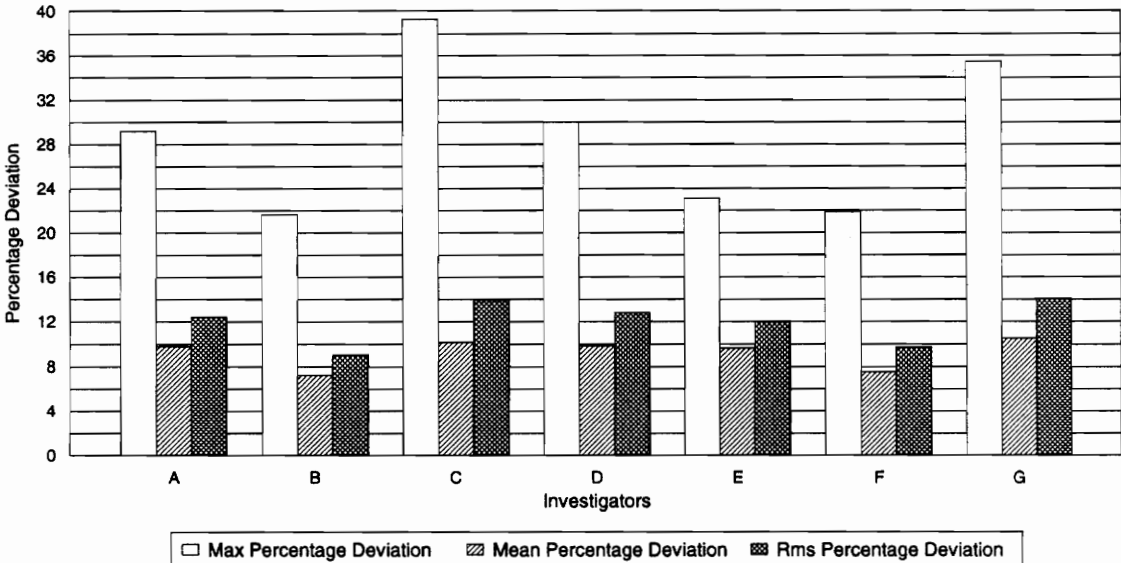
Difference (Deviation) between experimental and predicted values for Pitchwise Exit Circumferential Flow Angles Data



Notations for X-Axis: A = TRANSCode, B = TRACE_S (CH Grid), C = TRACE_S (OHHH Grid), D = Bassi-Savini, E = CANARI (K,Eps), F = CANARI (Michel), G = ADPAC

Figure 4.22: DLR Turbine Stator Test Case

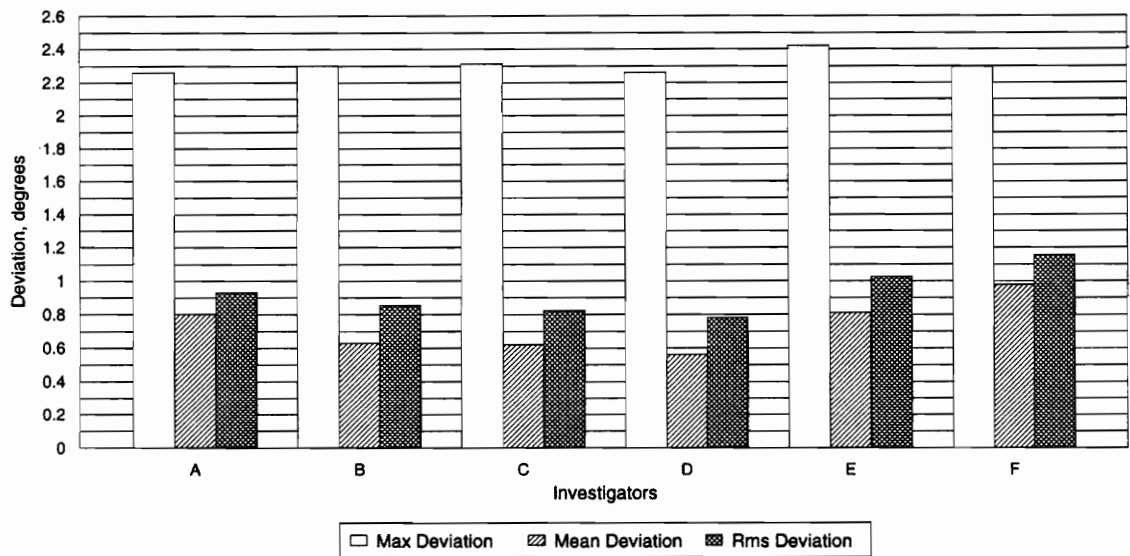
Percentage Difference (Deviation) between experimental and predicted values for Pitchwise Exit Circumferential Flow Angles Data



Notations for X-Axis: A = TRANSCode, B = TRACE_S (CH Grid), C = TRACE_S (OHHH Grid), D = Bassi-Savini, E = CANARI (K, Eps), F = CANARI (Michel), G = ADPAC

Figure 4.23: DLR Turbine Stator Test Case

Difference (Deviation) between experimental and predicted values for Pitchwise Exit Radial Flow Angles Data



Notations for X-Axis: A = TRANSCode, B = TRACE_S (CH Grid), C = TRACE_S (OHHH Grid), D = Bassi-Savini, E = CANARI (K, Eps), F = CANARI (Michel)

Figure 4.24: DLR Turbine Stator Test Case

Percentage Difference (Deviation) between experimental and predicted values for Pitchwise Exit Radial Flow Angles Data

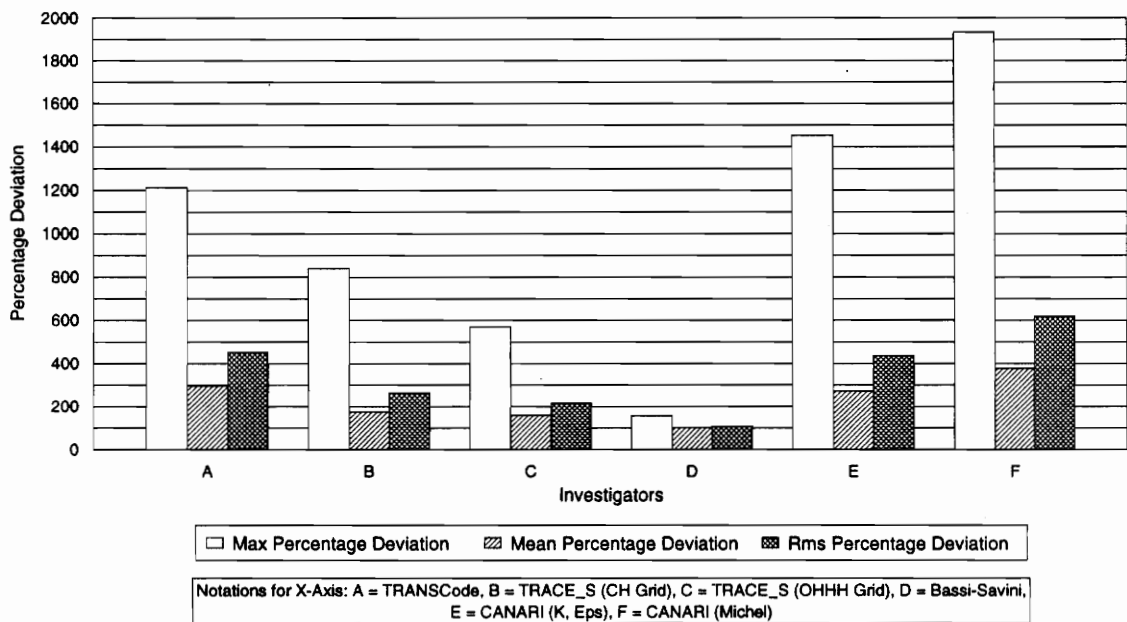
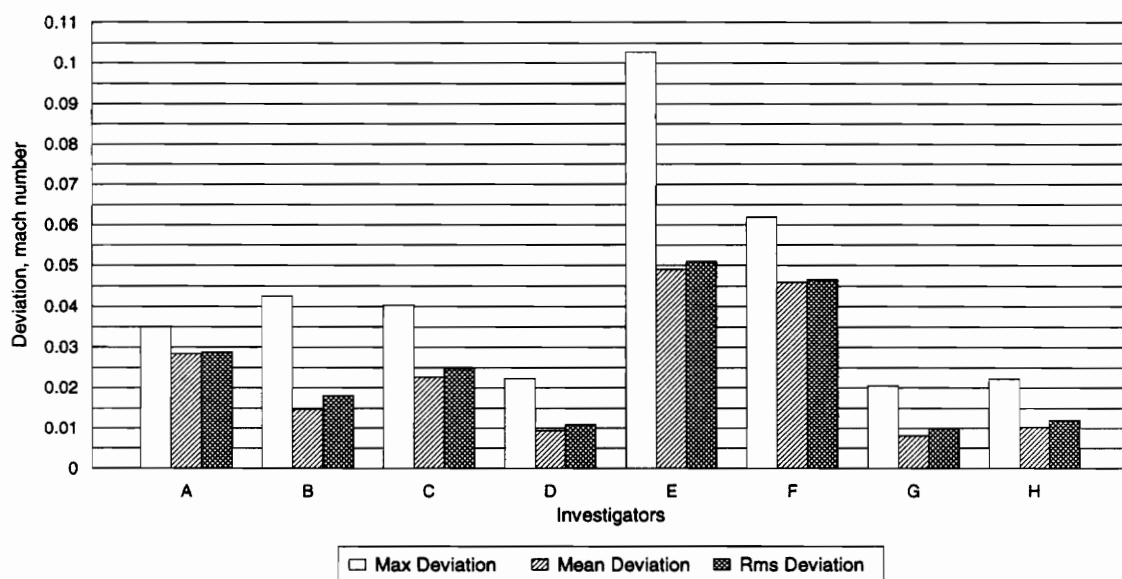


Figure 4.25: DLR Turbine Stator Test Case

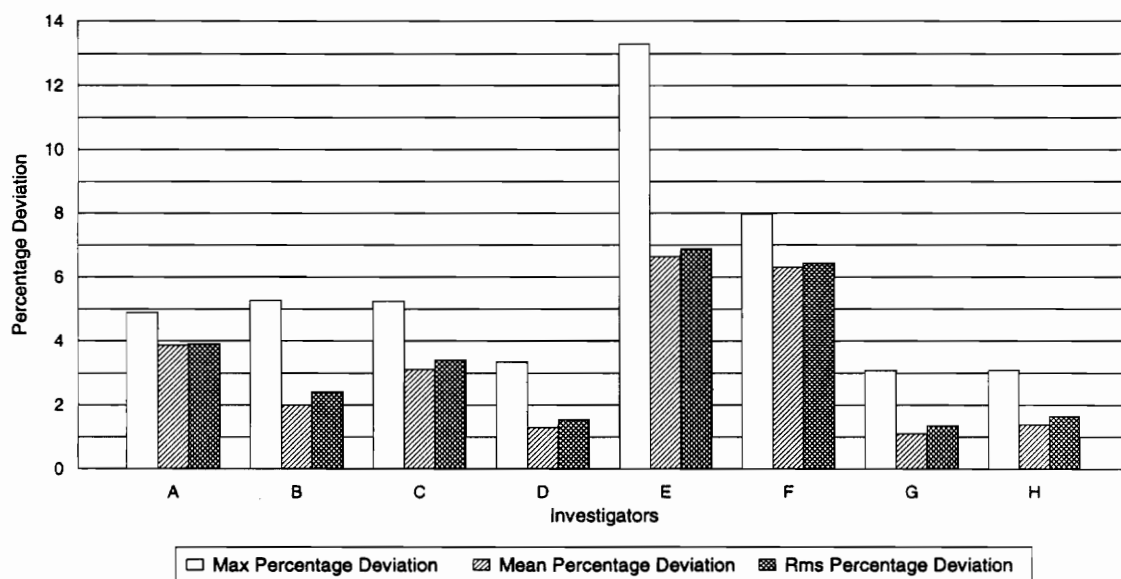
Difference (Deviation) between experimental and predicted values for Pitchwise Exit Mach Number Data



Notations for X-Axis: A = TRANSCoDe, B = TRACE_S (CH Grid), C = TRACE_S (OHMH Grid), D = Bassi-Savini, E = CANARI (K, Eps), F = CANARI (Michel), G = ADPAC, H = Dadone-DePalma

Figure 4.26: DLR Turbine Stator Test Case

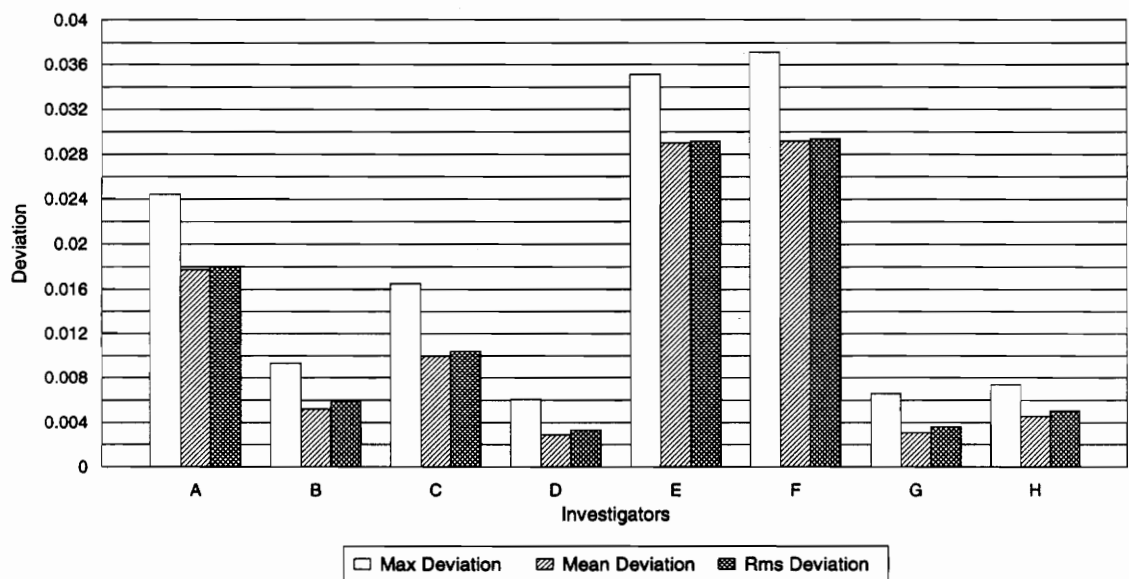
Percentage Difference (Deviation) between experimental and predicted values for Pitchwise Exit Mach Number Data



Notations for X-Axis: A = TRANSCoDe, B = TRACE_S (CH Grid), C = TRACE_S (OHHH Grid), D = Bassi-Savini, E = CANARI (K, Eps), F = CANARI (Michel), G = ADPAC, H = Dadone-DePalma

Figure 4.27: DLR Turbine Stator Test Case

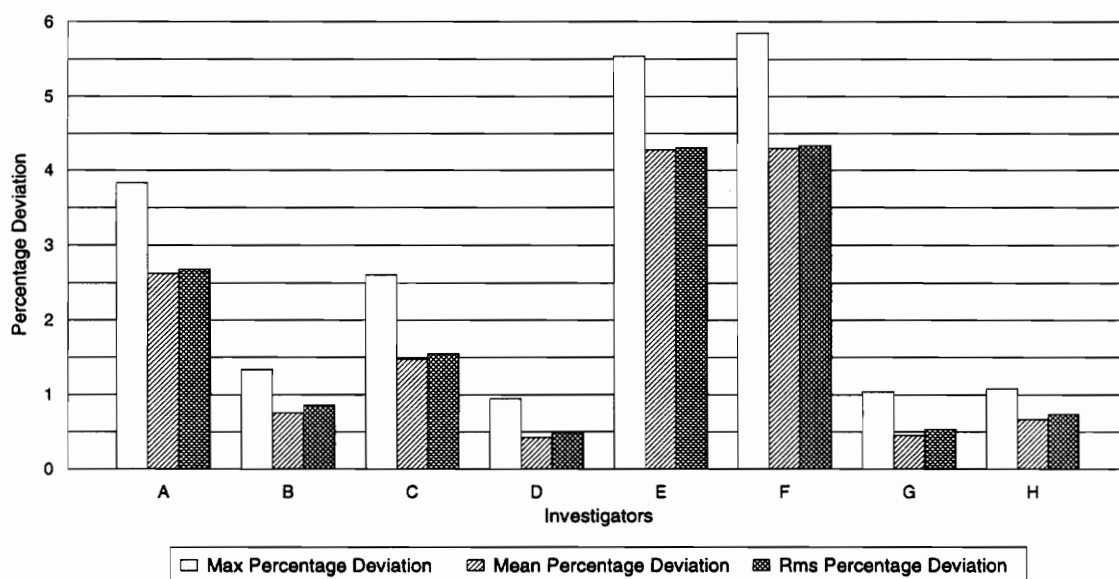
Difference (Deviation) between experimental and predicted values for Pitchwise Static Pressure Ratio Data



Notations for X-Axis: A = TRANSCODE, B = TRACE_S (CH Grid), C = TRACE_S (OHHH Grid), D = Bassi-Savini, E = CANARI (K, Eps), F = CANARI (Michel), G = ADPAC, H = Dadone - DePalma

Figure 4.28: DLR Turbine Stator Test Case

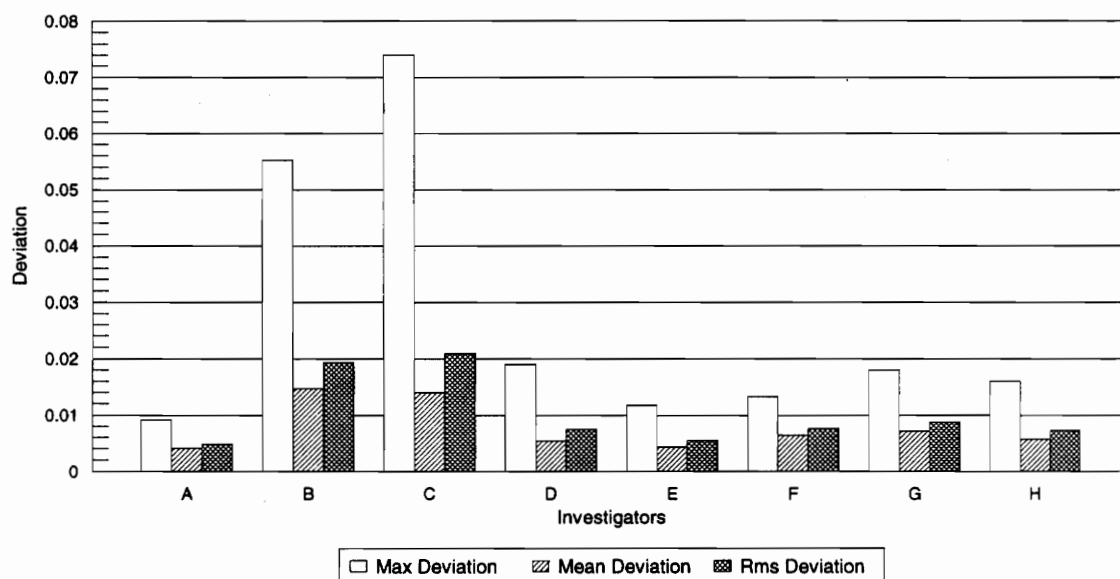
Percentage Difference (Deviation) between experimental and predicted values for Pitchwise Static Pressure Ratio Data



Notations for X-Axis: A = TRANSCoDe, B = TRACE_S (CH Grid), C = TRACE_S (OHHH Grid), D = Bassi-Savini, E = CANARI (K, Eps), F = CANARI (Michel), G = ADPAC, H = Dadone - DePalma

Figure 4.29: DLR Turbine Stator Test Case

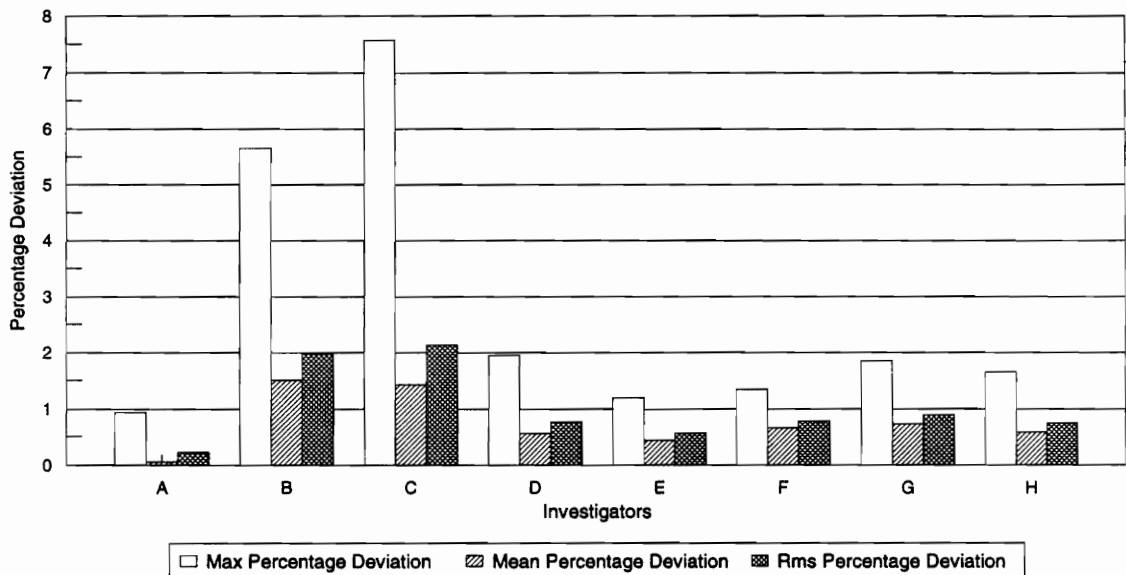
Difference (Deviation) between experimental and predicted values for Pitchwise Total Pressure Ratio Data



Notations for X-Axis: A = TRANSCoDe, B = TRACE_S (CH Grid), C = TRACE_S (OHHH Grid), D = Bassi-Savini, E = CANARI (K, Eps), F = CANARI (Michel), G = ADPAC, H = Dadone - DePalma

Figure 4.30: DLR Turbine Stator Test Case

Percentage Difference (Deviation) between experimental and predicted values for Pitchwise Total Pressure Ratio Data



Notations for X-Axis: A = TRANSCoDe, B = TRACE_S (CH Grid), C = TRACE_S (OHHH Grid), D = Bassi-Savini, E = CANARI (K, Eps), F = CANARI (Michel), G = ADPAC, H = Dadone - DePalma

Chapter 5: Discussion of Results

5.1 Discussion Overview

The purpose of this discussion is to indicate the prominent features in each set of results based on general observation. It is not an attempt by the author to rank the CFD codes based on the results presented. Although the focus of this chapter is on the maximum percentage deviation (maximum error) as they are widely used for comparison of results in engineering, the mean and rms values are included in this report to assist AGARD Working Group in their evaluation of the predicted results.

Table 5.1: Mean of the mean for the error analysis of NASA Rotor 37 Test Case

Figure No.	Mean of Max. Deviation	Mean of Mean Deviation	Mean of Max. % Deviation(error)	Mean of Mean % Deviation(error)
4.11, 4.12	0.0515	0.035	2.5235	1.6893
4.13, 4.14	0.0239	0.0181	2.6984	2.059
4.15, 4.16	0.1062	0.0528	5.0853	2.5534
4.17, 4.18	0.0476	0.0148	3.7142	1.1662
4.19, 4.20	0.0896	0.0205	11.8654	2.4723

Table 5.2: Mean of the mean for the error analysis of DLR Turbine Stator Test Case

Figure No.	Mean of Max. Deviation	Mean of Mean Deviation	Mean of Max. % Deviation(Error)	Mean of Mean % Deviation(Error)
4.21, 4.22	4.6944	1.7144	28.6208	9.2251
4.23, 4.24	2.3072	0.7313	1,025.7698	228.4069
4.25, 4.26	0.0434	0.0234	5.763	3.2044
4.27, 4.28	0.0178	0.0127	2.7751	1.8669
4.29, 4.30	0.027	0.0076	2.7679	0.7407

5.2 NASA Rotor 37 Test Case

The discussion of results in this section pertains to Figures 4.1 through 4.5 and Figures 4.11 through 4.20. For comparison of results, the mean of the mean is tabulated in Table 5.1. These mean or average values reflect the average of results over the number of data sets. For example, the “Mean of Max. Deviation” of 0.0515 in Table 5.1 represents the average of the eight different “Max. Deviation” values (hollow bars) in Figure 4.11. Similarly, the “Mean of Max. Percentage (%) Deviation” value of 2.5235 represents the average of the eight “Max. Percentage Deviation” values (hollow bars) in Figure 4.12.

The “Mean of Max. Deviation” in Table 5.1 seems to indicate that the CFD codes used in this validation exercise are capable of predicting the overall pressure ratio with an average maximum deviation of about 0.05 or 2.52% error. It is observed that the ADPAC, DRA TRANScode and Fottner-Hildebrandt’s TASCflow results show significant error compared to the other results. If these data were excluded, the mean of the maximum values in Table 5.1 would be 0.023 or 1.1%. The mean deviation would be 0.016 (or 0.78%) instead of 0.035 (or 1.69%).

For the overall efficiency results, the predicted data has an average of 0.0239 maximum deviation (or 2.7% error) or 0.0181 (or 2.059% error) of the mean deviation. Only two sets of data, CANARI’s Michel and κ, ϵ (listed as K,Eps in all figures and tables) models, show error above 3%. If both data were excluded in the computation, the mean of the maximum and mean deviation would be 0.0204 (2.3% error) and 0.0138 (1.58%).

Both the overall pressure and efficiency data show good correlation with the experimental data. However, it must be noted that the predictions from Couaillier's CANARI κ,ϵ model, Hutchinson and Ivanovich's TASCflow, and Fottner and Hildebrandt's TRACE_S have considerably fewer data points than the other four sets of data. Thus, any attempt to derive a conclusion from Figures 4.1 and 4.2 may be erroneous as the performance of a turbulence model may be misrepresented, like the CANARI κ,ϵ model which had only four data points on both overall performance plots.

In Figures 4.15 and 4.16, the maximum percentage error ranges between 3.04% and 6.42%. This is consistent with the comparison of overall performances in Figures 4.11 through 4.14. The mean of maximum percentage deviation shows a 5.0853% error. The average of the mean error for the pressure ratio results is 2.5534%. Similarly, the mean of the maximum and mean error are 3.7142% and 1.1662% for the Total Temperature Ratio comparison in Figures 4.17 and 4.18.

The adiabatic efficiency results in Figure 4.20 show that the maximum error ranges from 5.34% to 37.7% with the mean of about 11.9% (Table 5.1). The mean error ranges from 1.4% to 4% with an average of 2.5%.

5.3 DLR Turbine Stator Test Case

Table 5.2 lists the mean of the error analysis results of DLR Turbine Stator predictions. The average maximum error in predicting the exit circumferential angles is about 28.6% and average mean error is about 9.2%. These values appear to indicate that the CFD codes are mediocre for prediction of exit flow angles. The results for the exit radial flow angles appear to reconfirm this observation as the average maximum error in

the predictions is 1,025.8% and the mean of the mean error is 228.4%. The errors do not consistently occur at a certain location of the stator, unlike the results for the total temperature ratio in Figure 4.4 where codes yield maximal error at the tip and the hub of NASA Rotor 37 Test Case.

It must be noted that the exit radial flow angles are relatively small (less than 3 degrees) compared to the exit circumferential flow angles which are above 10 degrees. This may explain the large error encountered in the exit radial flow data.

The exit Mach number results show an average of 5.753% maximum error and 3.2044% mean error. If the CANARI κ, ϵ model values are omitted from the calculation, the resulting average for the maximum error is 4.69% and the mean error is 2.71%.

For the static pressure ratio data, the averages of the maximum and mean error are about 2.78% and 1.87% respectively. Note that the DRA TRANScode and both of CANARI's predictions account for most of the error in the averages in Table 5.2 as shown in Figures 4.27 and 4.28. With this observation, if their error are excluded in the computations for Table 5.2, the average of the maximum and mean error are about 1.4% and 0.75% respectively. These values and the original values are still small compared to the errors in the exit radial flow results.

Finally, in the total pressure ratio predictions, both TRACE_S predictions from Lisiewicz show a considerable amount of error. The average of the maximum and mean error are 2.77% and 0.74% respectively. These values are very low compared to other results for the DLR Turbine Stator Test Case. If the TRACE_S results were excluded in the values registered in Table 5.3, the average of the maximum and mean errors yield 1.49% and 0.5%.

5.4 Summary

The results for NASA Rotor 37 Test Case seem to indicate that the CFD codes used for the exercise are good predictors of overall performances for the NASA Rotor 37. The overall performance (overall pressure and efficiency) results yield an average maximum error of 2.47% for the overall pressure and 2.77% for the overall efficiency. As discussed in section 5.2, this observation may be misleading as some investigators used relatively fewer data points than others, like Couaillier (CANARI κ,ϵ data in Figures 4.1 and 4.2) who used only four data points for his predictions. Thus, the error associated with these data may not be as credible as data from ADPAC or TRANScode. Investigators from respective parties should be informed of such a discrepancy and they should be encouraged to generate more data points for a better comparison with other codes or turbulence models.

Other results for the NASA Rotor 37 test case are consistent except for the adiabatic efficiency which yields predictions of slightly above 10%. Predictions from ADPAC, TASCflow (ASC's results), CANARI's Michel model with H-O-H grid, and Fottner and Hildebrandt's TASCflow results produced errors above 10% while the results from CANARI κ,ϵ model show errors above 27%.

Of the five sets of data in the DLR Turbine Stator Test Case, the exit circumferential and radial flow angles are the most difficult properties to predict. These results have as high as 1900% error as shown in Figure 4.24. These observations indicate that the flow angle results are not reliable.

The results for the exit Mach number, static pressure ratio and total pressure ratio yield error below 10% except for the CANARI κ,ϵ model which registers over-predictions for the exit Mach number of approximately 13% (Figure 4.26).

The panel of experts in WG-26 initially predicted that the results from this exercise would yield a 10% error margin for the CFD codes. The above summary indicates that, with certain exceptions, the findings for this exercise are consistent with the Working Group's predictions.

Chapter 6: Conclusions and Recommendations

6.1 Conclusions

A method of comparison between data was designed so that the Working Group can better discuss the differences in models and grids used in their results. The internet was the primary method of collecting the data from investigators who are both international and domestic, and this method proved to be very efficient and effortless.

A visualization software, TECPLOT, was adopted and used by the author to produce overplots of the experimental results and investigator predictions. With a common axis, experimental results from the two test cases were successfully overlaid with the results from investigators of WG-26. These plots help investigators to visualize the differences between their codes and compare results.

Finally, a simple error analysis which emphasized the key features or differences in each data set was performed. This analysis yielded results that were consistent with the Working Group's initial predictions of an error margin of 10% from the CFD codes.

6.2 Recommendations

The predictions from investigators are constantly being updated and new results are still being collected as of this report. The following steps may be implemented to ease the data collection and plotting processes.

1. The current FTP software is not compatible with the operating systems on the computers in the Virginia Tech Turbomachinery Laboratory. The laboratory should consider installing new versions of FTP software to facilitate the data collection process.

2. A detailed description of the data format should be sent all investigators so as to reduce the time spent on manipulating data for plotting. A sample of a TECPLOT data file can also be attached to the description for reference.
3. Other statistical approach to analyze the error of the results like χ^2 may be used in place of the method discussed in this report. This may provide a better form of error comparison and better understanding of the data.

There are several interesting observations that may require further investigation. These observations are listed below.

1. There is consistent under-prediction of overall efficiency for the NASA Rotor 37 Test Case as shown in Figure 4.2.
2. Except for the CANARI predictions, the predictions are mostly over-predicting the overall pressure ratio values.
3. CFD codes used in this exercise are poor predictors for the exit radial flow angles of DLR Turbine Stator Test Case as illustrated in Figure 4.7.
4. There is an exaggerated boundary layer separation effect on the total pressure and total temperature values for the hub of the DLR Turbine Stator Test Case. This is illustrated in Figures 4.3 and 4.4.
5. Predictions at mid-span for most DLR results are not accurate for some codes. An investigation of the grid geometry around the mid-span may be performed so as to modify the existing geometry used by the investigators and rectify this inaccuracy.

References

1. Barber, T.J., D. Choi, R.A. Delaney, E.J. Hall, G.S. McNulty, "Preliminary Findings in Certification of ADPAC," AIAA 94-2240, 25th AIAA Fluid Dynamics Conference, Colorado Springs, CO, 1994.
2. Celestina, M.L. and K.L. Suder, "Experimental and Computational Investigation of the Tip Clearance Flow in a Transonic Axial Compressor Rotor," paper presented at the 39th ASME International Gas Turbine and Aeroengine Congress and Exposition, The Hague, June 1994.
3. Chima, R.V., K.L. Suder and A.J. Strazisar, "The Effect of Adding Roughness and Thickness to a Transonic Axial Compressor Rotor," paper presented at the 39th ASME International Gas Turbine and Aeroengine Congress and Exposition, The Hagu, June 1994.

APPENDIX A: Illustrations for Circumferential Flow Angle and Radial Flow Angle

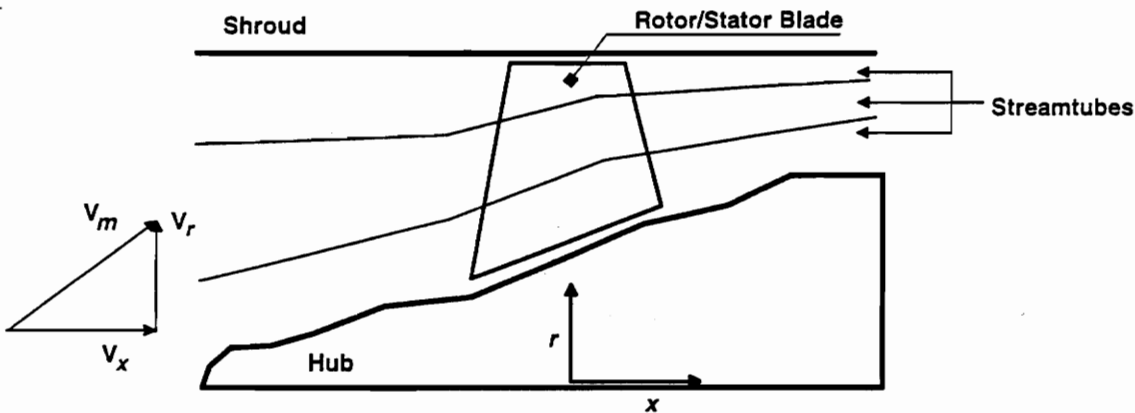


Figure A.1: Front View of Axial Flow Machinery with Radial Flow Angle, ϕ .
(V_m , V_r and V_x in the velocity triangle are absolute meridional, radial and axial velocities respectively.)

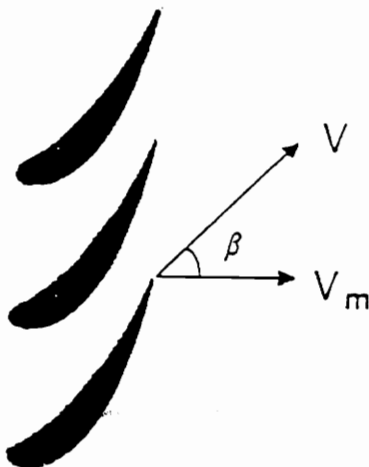


Figure A.2: Velocity Triangle and Circumferential Flow Angle, β , at the Exit of Turbine Stator (V and V_m refer to the absolute velocity and meridional velocity of flow).

APPENDIX B: Sample code in Fortran for Data Manipulation and Sample Data File in TECPLOT Format

APPENDIX B.1: List of sample code in Fortran for Data Manipulation

```
cc      Filename: data.for
cc
cc      Input/Data Filename: temp.dat
cc
cc      Output Filename: out.dat
cc
cc      Author: Jeremy Chan
c
c      This program flip-flops the columns of data file
c
c      INTEGER I,K,L,COL,BLOCK
c      REAL u(10,100)
c
c      Enter the # of blocks for the data files
c
c      BLOCK = 9
c
c      Enter the # of columns for the data files
c
c      COL=37
c      OPEN (55,FILE='temp.dat',status='old')
c      OPEN (20,FILE='out.dat',status='unknown')
c
c      Do-Loop to read the independent variables
c
c      DO 20 I=1,BLOCK
c
c      Internal Do-Loop to read data in row-wise format
c
c          READ (55,*) (u(I,K),K=1,COL,1)
20      CONTINUE
c
c      Do-Loop to write the data into output file
c      in two columns; independent and the corresponding
c      dependent variables
c
c      DO 35 K=2,BLOCK
c          DO 34 I=1,COL
c              WRITE (20,110) u(K,I), u(1,I)
34      CONTINUE
35      CONTINUE
c
c      Output format for the output file
c
110     FORMAT ('',F13.6,1x,F10.6)
c
c      Closing all data files
c
c      CLOSE (55)
c      CLOSE (20)
c      END
c
c      End of program
c
```

APPENDIX B.2: Sample Data File in TECPLOT Format

TITLE = "Experimental Data of Overall Pressure Ratio vs. Corrected Flow"

VARIABLES = "Corrected Flow", "Overall Pressure Ratio"

ZONE T = "Experimental", F=POINT

0.997659298	1.995
0.994386649	2.018
0.987407889	2.065
0.980450802	2.084
0.962050282	2.11
0.946315561	2.135
0.926462939	2.144

ZONE T = "ADPAC (Delaney & McNulty, Allison)", F=POINT

0.99514521	1.9691
0.993671435	2.0363
0.992262679	2.0854
0.990940616	2.1117
0.987928045	2.1381
0.980905938	2.1617
0.966666667	2.1793
0.956285219	2.1863
0.951452102	2.1899
0.944191591	2.1919
0.937407889	2.1938
0.930689207	2.1913
0.92496749	2.187
0.922388383	2.1839

ZONE T = "TASCFLOW (Hutchinson, ASC)", F=POINT

0.925	2.15908
0.953	2.13315
0.98	2.11779
0.993	2.07309

ZONE T = "DRA TRANSCODE (Calvert, DRA)", F=POINT

1	1.8255
0.9999	1.8991
0.9992	1.9915
0.998	2.0433
0.9963	2.0963
0.9885	2.1467
0.9803	2.1635
0.9746	2.1706
0.9578	2.1611
0.9537	2.1685
0.9483	2.1701
0.9418	2.171

0.9343	2.1715
0.9279	2.1703
ZONE T="CANARI Michel Prediction (HOH-Grid)"	
0.95	2.0692
0.958	2.094
0.979	2.067
0.982	2.061
0.991	2.03
0.997	1.978
0.999	1.951
1	1.94
ZONE T="CANARI K,Eps Prediction (OH-Grid)"	
0.9759	2.115
0.9808	2.098
0.9841	2.071
0.9936	1.995
ZONE T="TRACE_S 500K-GRID"	
9.830000E-01	2.082000
9.810000E-01	2.085000
9.710000E-01	2.100000
9.640000E-01	2.110000
9.410000E-01	2.121000
9.240000E-01	2.129000
ZONE T="TASCflow 72K-GRID"	
9.900000E-01	2.147000
9.800000E-01	2.163000
9.700000E-01	2.164000
9.620000E-01	2.163000
9.460000E-01	2.159000
9.340000E-01	2.154000
9.250000E-01	2.149000

Appendix C: Tables of Linearly Interpolated Data for Error Analysis

Table C.1: Linearly interpolated data from Overall Pressure vs. Normalized Mass Flow data for NASA Rotor 37 using TECPLOT.

No.	Span (%)	Experimental Data	ADPAC	ASC TASCflow	DRA TRANScode	CANARI Michel (HOH Grid)	CANARI K.Eps (OH Grid)	Fottner/Hildebrandt	
								TRACE_S	TASCflow
1	0.9976593	1.950000			2.053920	1.969100			
2	0.99438665	2.018000	2.003690		2.108660	2.006500			
3	0.98740789	2.065000	2.139850	2.092320	2.148940	2.042370	2.044540		2.151150
4	0.98045082	2.084000	2.162260	2.116240	2.163190	2.064100	2.099210	2.085820	2.162280
5	0.96205028	2.110000	2.182410	2.128000	2.163500	2.088979		2.110930	2.163010
6	0.94631556	2.135000	2.191310	2.139340	2.170370			2.118460	2.159080
7	0.92646294	2.144000	2.188120	2.157730				2.127840	2.149810

Table C.2: Linearly interpolated data from Overall Efficiency vs. Normalized Mass Flow data for NASA Rotor 37 using TECPLOT.

No.	Span (%)	Experimental Data	ADPAC	ASC TASCflow	DRA TRANScode	CANARI Michel (HOH Grid)	CANARI K.Eps (OH Grid)	Fottner/Hildebrandt	
								TRACE_S	TASCflow
1	0.997659	0.890000			0.866362	0.858304			
2	0.994387	0.891000	0.867069		0.869808	0.858657			
3	0.987408	0.887000	0.876507	0.864840	0.868081	0.857163	0.853896		0.876823
4	0.980451	0.879000	0.873876	0.862887	0.864772	0.854484	0.855293	0.866120	0.872857
5	0.962050	0.875000	0.864743	0.855155	0.852687	0.846736		0.856910	0.860833
6	0.946316	0.862000	0.856841	0.847835	0.842031			0.849727	0.851291
7	0.926463	0.848000	0.846336	0.837483				0.839347	0.839262

Table C.3: Linearly interpolated data from Total Pressure Ratio vs. Percentage Span data for NASA Rotor 37 using TECPLOT.

No.	Span (%)	Experimental Data	ADPAC	ASC TASCflow	DRA TRANScode	CANARI Michel (HOH Grid)	CANARI K.Eps (OH Grid)	Fottner/Hildebrandt	
								TRACE_S	TASCflow
1	5	2.119600	2.255900	2.182490	2.182510	2.202420	2.184190	2.229690	2.244540
2	10	2.108700	2.221610	2.183210	2.220960	2.160070	2.162700	2.168000	2.207510
3	15	2.104000	2.205570	2.177450	2.217420	2.138490	2.153040	2.137090	2.190230
4	20	2.108100	2.195880	2.173220	2.208540	2.130410	2.151650	2.121450	2.183530
5	25	2.118900	2.189040	2.169110	2.199390	2.127030	2.152810	2.113410	2.180600
6	30	2.133900	2.182950	2.164370	2.191380	2.123740	2.152940	2.110260	2.179170
7	37	2.145500	2.174940	2.155790	2.180740	2.116380	2.146540	2.109810	2.178320
8	44	2.136000	2.167150	2.143920	2.168440	2.104670	2.131140	2.107630	2.178610
9	51	2.117600	2.159310	2.128360	2.158310	2.088920	2.109960	2.099230	2.177700
10	58	2.087600	2.151380	2.112400	2.149150	2.069590	2.088210	2.083870	2.172800
11	65	2.064500	2.143280	2.100120	2.140380	2.047580	2.070940	2.060660	2.163140
12	70	2.055700	2.136950	2.095270	2.135470	2.030960	2.064030	2.042400	2.154590
13	75	2.050900	2.130260	2.092860	2.130160	2.013460	2.059970	2.026980	2.146360
14	80	2.040000	2.122960	2.091550	2.123740	1.993750	2.056820	2.017820	2.138610
15	85	2.031800	2.113980	2.088880	2.115880	1.969070	2.051750	2.014760	2.128490
16	90	2.010800	2.101410	2.077520	2.104430	1.937890	2.039690	2.007510	2.113780
17	94	1.991000	2.080730	2.049930	2.082300	1.906730	2.019070	1.991330	2.093910
18	97	1.959700	2.039530	1.992480	2.026680	1.840020	1.989120	1.971170	2.042000

Table C.4: Linearly interpolated data from Total Temperature Ratio vs. Percentage Span data for NASA Rotor 37 using TECPLOT.

No.	Span (%)	Experimental Data	ADPAC	ASC TASCflow	DRA TRANScode	CANARI Michel (HOH Grid)	CANARI K.Eps (OH Grid)	Fottner/Hildebrandt	
								TRACE_S	TASCflow
1	5	1.255700	1.279200	1.276170	1.279960	1.265150	1.267530	1.268820	1.288250
2	10	1.253400	1.271040	1.272940	1.275990	1.257270	1.259560	1.258350	1.273920
3	15	1.254900	1.269430	1.272600	1.274700	1.256840	1.259670	1.254580	1.270240
4	20	1.255900	1.269790	1.273700	1.274950	1.258120	1.262110	1.253990	1.270410
5	25	1.258600	1.271170	1.275290	1.275780	1.259860	1.265060	1.255160	1.271760
6	30	1.263400	1.272730	1.276670	1.276690	1.261570	1.267790	1.257170	1.273430
7	37	1.271500	1.274890	1.278180	1.278980	1.263630	1.270490	1.260520	1.276260
8	44	1.270600	1.276680	1.279070	1.280870	1.264940	1.271600	1.263650	1.279750
9	51	1.268800	1.277750	1.279050	1.282620	1.265110	1.271420	1.265860	1.283200
10	58	1.264800	1.278550	1.278510	1.283600	1.263940	1.270670	1.266610	1.285660
11	65	1.260500	1.279160	1.278310	1.283590	1.261960	1.270340	1.265460	1.286760
12	70	1.260900	1.280020	1.278560	1.283220	1.260980	1.271270	1.264140	1.286890
13	75	1.262700	1.281530	1.279100	1.283010	1.261150	1.273520	1.263870	1.287020
14	80	1.263400	1.284120	1.280290	1.284690	1.263320	1.277730	1.266950	1.288040
15	85	1.273400	1.289870	1.283260	1.290830	1.269530	1.285290	1.276460	1.295010
16	90	1.277300	1.300280	1.289500	1.305870	1.284010	1.299350	1.294490	1.311450
17	94	1.284100	1.316500	1.289860	1.325510	1.309560	1.316800	1.314030	1.317580
18	97	1.283300	1.337000	1.276260	1.344600	1.351920	1.332640	1.328760	1.305470

Table C.5: Linearly interpolated data from Adiabatic Efficiency vs.Percentage Span data for NASA Rotor 37 using TECPLOT.

No.	Span (%)	Experimental Data	ADPAC	ASC TASCflow	DRA TRANScode	CANARI Michel (HOH Grid)	CANARI K.Eps (OH Grid)	Fotmer/Hildebrandt	
								TRACE_S	TASCflow
1	5	0.936300	0.937255	0.904544	0.893468	0.954447	0.934829	0.982316	0.921859
2	10	0.937600	0.945117	0.915677	0.929037	0.956684	0.949897	0.956891	0.930134
3	15	0.929000	0.941150	0.913359	0.931445	0.944403	0.943377	0.942781	0.924345
4	20	0.928000	0.934055	0.906881	0.925226	0.934519	0.933755	0.934479	0.918655
5	25	0.925300	0.925187	0.899481	0.917014	0.926109	0.924095	0.925311	0.912402
6	30	0.918000	0.916253	0.892168	0.908281	0.917947	0.914729	0.916152	0.906362
7	37	0.897700	0.904273	0.882227	0.895566	0.906133	0.901667	0.904508	0.898073
8	44	0.894800	0.893797	0.872402	0.882304	0.894212	0.888571	0.893193	0.889166
9	51	0.889400	0.885692	0.863176	0.870944	0.883614	0.876123	0.881861	0.879845
10	58	0.883800	0.878447	0.855187	0.862589	0.875110	0.865041	0.872417	0.871210
11	65	0.883400	0.871739	0.848508	0.857481	0.867410	0.855259	0.863776	0.863391
12	70	0.876300	0.865309	0.844807	0.855871	0.859716	0.848016	0.855688	0.858001
13	75	0.867100	0.856747	0.841710	0.853322	0.847620	0.838521	0.844398	0.852130
14	80	0.857700	0.844636	0.837372	0.844501	0.827686	0.823945	0.828399	0.844327
15	85	0.821200	0.822741	0.827005	0.822258	0.792683	0.799054	0.801488	0.822313
16	90	0.796600	0.787188	0.802555	0.775804	0.732843	0.754733	0.757372	0.781693
17	94	0.765400	0.736057	0.785293	0.717459	0.654455	0.701849	0.724309	0.778951
18	97	0.748100	0.670334	0.788019	0.649889	0.541110	0.652717	0.716771	0.811023

Table C.6: Linearly interpolated data from Pitchwise Exit Circumferential Flow Angles data for DLR Turbine Stator using TECPLOT.

No.	Span(%)	Experimental	DRA TRANScode	TRACE_S (CH GRID)	TRACE_S (OHHH GRID)	Bassi-Savini	CANARI K.Eps	CANARI Michel	ADPAC
1	5.858856	27.267400	27.201800	23.321300	23.454800	22.383600	22.312100	22.114100	22.286600
2	9.364696	27.423300	23.252100	24.990100	24.078500	23.020700	22.662300	23.234800	22.252200
3	12.847078	26.506700	22.797500	25.691200	24.621600	22.839400	22.592900	23.332700	22.130200
4	16.400000	24.592600	22.137100	25.006300	24.033900	22.325600	22.217400	22.877600	21.965900
5	19.952930	23.006300	21.479900	23.512300	22.574000	21.789700	21.748600	22.243600	21.762000
6	24.611770	21.939900	20.801300	22.182200	21.384700	21.145600	21.156300	21.490400	21.395200
7	34.023555	20.439800	19.838800	21.078100	20.472600	20.218200	20.149500	20.567500	20.570900
8	43.482357	18.937600	19.034700	20.072800	19.685100	19.603000	19.405600	20.201600	19.787200
9	55.270610	18.889700	18.247700	18.634800	18.673500	19.101900	18.815600	19.939000	19.109400
10	64.688235	19.165900	17.920400	19.728200	19.738500	18.725100	18.598200	19.499900	18.713200
11	69.364680	19.213500	17.969000	19.988200	20.565200	18.522000	18.546500	19.071200	18.483400
12	72.870597	18.408700	18.114100	19.595900	20.527800	18.323300	18.516800	18.624500	18.289300
13	76.447050	17.037300	18.257700	18.820300	19.522100	18.120600	18.424100	17.984200	18.051000
14	79.976486	16.111300	18.244400	17.954700	18.155100	17.842400	18.217600	17.261800	17.759600
15	83.482330	15.650800	17.926900	17.037900	17.128300	17.541200	17.809500	16.502100	17.419100
16	87.058815	14.763000	17.229600	16.016600	16.829000	17.090300	17.042500	15.759700	17.035400
17	90.517639	13.263200	16.217200	15.089100	16.692200	16.409700	15.858300	15.077400	16.585100
18	94.070564	11.660600	15.061300	14.182300	16.240900	15.154400	14.350000	14.206300	15.790500

Table C.7: Linearly interpolated data from Pitchwise Exit Radial Flow Angles data for DLR Turbine Stator using TECPLOT

No.	Span(%)	Experimental	DRA TRANScode	TRACE_S (CH GRID)	TRACE_S (OHHH GRID)	Bassi-Savini	CANARI K.Eps	CANARI Michel
1	5.858856	0.836187	0.165765	0.122167	0.219710	0.095188	0.219634	0.208103
2	9.364696	1.351197	0.126647	0.093020	0.227040	0.096120	0.202167	0.092744
3	12.847078	0.824715	0.055092	-0.115846	0.013341	0.088962	0.110127	-0.080950
4	16.400000	-0.130181	-0.123301	-0.326316	-0.007783	0.071855	-0.003100	-0.252865
5	19.952930	-0.485689	-0.244752	-0.428553	-0.105555	0.073899	-0.100311	-0.359899
6	24.611770	-0.275324	-0.448409	-0.357533	-0.081850	0.070720	-0.209147	-0.401378
7	34.023555	-0.164397	-0.741123	-0.291855	-0.079955	0.036317	-0.413090	-0.423425
8	43.482357	-0.255602	-0.939927	-0.308783	-0.164311	0.035822	-0.545726	-0.587467
9	55.270610	-0.078812	-1.033430	0.074915	0.110112	-0.009557	-0.638647	-0.914563
10	64.688235	-0.492209	-0.996780	-0.410783	-0.037116	-0.059484	-0.711226	-1.217680
11	69.364680	-0.283638	-1.006300	-0.696551	-0.537880	-0.081517	-0.777766	-1.358550
12	72.870597	-0.120398	-1.002220	-0.757315	-0.757079	-0.087405	-0.857005	-1.495510
13	76.447050	-0.254545	-0.981698	-0.728724	-0.699342	-0.093412	-0.977573	-1.474980
14	79.976486	-0.069919	-0.832739	-0.655845	-0.466835	-0.121814	-1.083170	-1.421680
15	83.482330	0.378613	-0.652457	-0.539748	-0.326901	-0.149967	-1.114690	-1.273640
16	87.058815	0.765559	-0.322040	-0.377149	-0.325899	-0.147222	-0.964781	-0.992902
17	90.517639	0.973573	-0.124541	-0.209954	-0.246401	-0.106460	-0.597499	-0.567542
18	94.070564	2.256616	-0.001733	-0.042654	-0.053482	-0.003701	-0.163892	-0.038334

Table C.8: Linearly interpolated data from Pitchwise Exit Mach Number data for DLR Turbine Stator using TECPLOT.

No.	Span(%)	Experimental	DRA TRANSCODE	TRACE_S (CH GRID)	TRACE_S (OHHH GRID)	Bassi- Savini	CANARI K.Eps	CANARI Michel	ADPAC	Dadone- De-Palma
1	5.858856	0.808516	0.775909	0.765974	0.768267	0.817791	0.856816	0.870312	0.813561	0.818431
2	9.364696	0.801823	0.769866	0.794748	0.835004	0.803304	0.854776	0.845442	0.810928	0.820998
3	12.847078	0.790788	0.765058	0.773507	0.818701	0.796329	0.847098	0.834070	0.804889	0.812945
4	16.400000	0.791296	0.763923	0.760878	0.793682	0.791523	0.842464	0.830081	0.797961	0.802283
5	19.952930	0.793995	0.763344	0.770512	0.795653	0.786776	0.838804	0.828518	0.790602	0.794318
6	24.611770	0.794211	0.759297	0.788020	0.810427	0.780288	0.832585	0.825504	0.780861	0.784612
7	34.023555	0.772401	0.742378	0.772282	0.792905	0.765950	0.875121	0.811302	0.761887	0.766483
8	43.482357	0.754677	0.725430	0.754651	0.773012	0.751427	0.795871	0.791801	0.744774	0.752361
9	55.270610	0.720680	0.705327	0.731020	0.747199	0.734506	0.772985	0.770670	0.725869	0.737562
10	64.688235	0.709735	0.686860	0.715866	0.727369	0.721536	0.755470	0.757978	0.713124	0.723288
11	69.364680	0.707468	0.677502	0.714274	0.728353	0.715253	0.747700	0.753006	0.707856	0.715874
12	72.870597	0.698846	0.671473	0.711864	0.724537	0.710863	0.742669	0.749855	0.704338	0.710142
13	76.447050	0.696668	0.666799	0.710089	0.717145	0.706386	0.738917	0.746908	0.701249	0.704294
14	79.976486	0.697563	0.663519	0.709199	0.713977	0.702752	0.735894	0.743790	0.698840	0.699220
15	83.482330	0.692896	0.660716	0.706971	0.714104	0.699293	0.733100	0.740192	0.696696	0.694410
16	87.058815	0.683228	0.657139	0.702222	0.713967	0.696194	0.729516	0.735577	0.694667	0.690789
17	90.517639	0.675546	0.651173	0.696240	0.710916	0.692812	0.723992	0.729323	0.692319	0.687720
18	94.070564	0.666055	0.639468	0.687476	0.696955	0.688253	0.713003	0.717796	0.686453	0.686514

Table C.9: Linearly interpolated data from Pitchwise Static Pressure Ratio data for DLR Turbine Stator using TECPLOT.

No.	Span(%)	Experimental	DRA TRANSCODE	TRACE_S (CH GRID)	TRACE_S (OHHH GRID)	Bassi- Savini	CANARI K.Eps	CANARI Michel	ADPAC	Dadone- De-Palma
1	5.858856	0.634243	0.649057	0.626314	0.617753	0.631364	0.599159	0.597127	0.627687	0.627415
2	9.364696	0.635704	0.653042	0.630293	0.622280	0.635304	0.603933	0.603344	0.632255	0.631266
3	12.847078	0.636152	0.657044	0.633955	0.626518	0.639129	0.608271	0.608271	0.636378	0.635638
4	16.400000	0.636934	0.661339	0.637150	0.630217	0.642968	0.612065	0.612065	0.640566	0.640466
5	19.952930	0.642133	0.665387	0.640829	0.634209	0.646953	0.615736	0.615736	0.644824	0.645470
6	24.611770	0.648991	0.670973	0.646684	0.640131	0.652056	0.621080	0.621080	0.650461	0.651973
7	34.023555	0.663562	0.682900	0.659211	0.653694	0.662887	0.634028	0.634028	0.662408	0.665224
8	43.482357	0.673937	0.692128	0.668622	0.663723	0.671925	0.644178	0.644178	0.671748	0.674695
9	55.270610	0.689488	0.704367	0.680993	0.677082	0.684968	0.657308	0.657309	0.684069	0.683774
10	64.688235	0.699034	0.713564	0.689750	0.686025	0.694377	0.667159	0.667159	0.693533	0.692041
11	69.364680	0.702496	0.717889	0.694424	0.690845	0.698917	0.671928	0.671928	0.698063	0.696229
12	72.870597	0.706642	0.721058	0.697839	0.694690	0.702177	0.675469	0.675469	0.701427	0.699269
13	76.447050	0.709331	0.724131	0.701586	0.698144	0.705503	0.679136	0.679136	0.704901	0.702371
14	79.976486	0.711749	0.727278	0.705080	0.701561	0.708991	0.682808	0.682808	0.708400	0.705322
15	83.482330	0.714610	0.730237	0.708701	0.705342	0.712472	0.686507	0.686507	0.711760	0.708263
16	87.058815	0.717067	0.733659	0.712466	0.709699	0.715896	0.690287	0.690287	0.715105	0.711547
17	90.517639	0.718554	0.736862	0.716048	0.713813	0.719218	0.693886	0.693886	0.718342	0.715166
18	94.070564	0.721728	0.740061	0.719752	0.717599	0.722611	0.697606	0.697606	0.721981	0.719379

Table C.10: Linearly interpolated data from Pitchwise Total Pressure Ratio data for DLR Turbine Stator using TECPLOT.

No.	Span(%)	Experimental	DRA TRANSCODE	TRACE_S (CH GRID)	TRACE_S (OHHH GRID)	Bassi- Savini	CANARI K.Eps	CANARI Michel	ADPAC	Dadone- De-Palma
1	5.858856	0.976737	0.967801	0.921515	0.902773	0.979727	0.967801	0.978317	0.973329	0.974644
2	9.364696	0.973039	0.968129	0.954999	0.970497	0.971608	0.973431	0.963089	0.977138	0.982963
3	12.847078	0.965911	0.969291	0.943210	0.961500	0.970710	0.972840	0.959645	0.977184	0.981860
4	16.400000	0.967705	0.974110	0.936867	0.945208	0.971919	0.975027	0.961696	0.976575	0.978929
5	19.952930	0.976010	0.979200	0.948187	0.951972	0.973389	0.978323	0.965920	0.975733	0.978781
6	24.611770	0.984521	0.983475	0.970628	0.973684	0.974872	0.981497	0.971314	0.974739	0.979202
7	34.023555	0.983927	0.983441	0.972546	0.975653	0.975846	0.982863	0.975532	0.972751	0.980007
8	43.482357	0.984456	0.982781	0.971748	0.973808	0.977139	0.981737	0.974020	0.972177	0.982269
9	55.270610	0.977482	0.982129	0.968572	0.969966	0.980437	0.980280	0.973608	0.972772	0.981628
10	64.688235	0.980514	0.978950	0.967558	0.965193	0.982101	0.978847	0.976248	0.974924	0.980542
11	69.364680	0.982859	0.976982	0.972299	0.972442	0.982875	0.978701	0.978601	0.976377	0.979825
12	72.870597	0.980932	0.976246	0.974640	0.974260	0.983540	0.979201	0.980835	0.977953	0.979035
13	76.447050	0.982236	0.978461	0.977741	0.972172	0.984218	0.980906	0.983422	0.980056	0.978230
14	79.976486	0.985605	0.977870	0.981581	0.973671	0.985862	0.983196	0.985849	0.982789	0.977927
15	83.482330	0.985200	0.979386	0.984404	0.978765	0.987647	0.985669	0.987860	0.985567	0.977850
16	87.058815	0.980041	0.980889	0.985306	0.984628	0.989659	0.987514	0.989039	0.988453	0.979327
17	90.517639	0.975726	0.980196	0.984943	0.987701	0.991275	0.987410	0.988454	0.990931	0.981482
18	94.070564	0.973002	0.974925	0.982526	0.981186	0.991953	0.982740	0.983308	0.990948	0.986761

Vita

Chun Ngok Chan was born August 20, 1970 in the Republic of Singapore. Growing up in the island city, he attended Catholic Junior College, a state-run pre-university established by the order of the Christian Brothers. Though a devoted Buddhist, his parents entrusted him to a Catholic institution of higher learning because of its Catholic values and motivating academia. Upon graduation, he served an army signal unit in the Singapore Armed Forces. After completing his 30 months' service, he pursued a Bachelor of Science degree in Mechanical Engineering at Christian Brothers University in Memphis, Tennessee. He graduated in May 1995 and ascended to a Master of Engineering program at Virginia Tech. He intends to pursue a career in Process Engineering upon his graduation.